INVESTIGATION OF BOUNDARY LAYER RELAMINARIZATION ON A REENTRY VEHICLE NOSETIP

Calvin J. Wolf, et al

Acurex Corporation

Prepared for:

Naval Ordnance Laboratory

May 1975

AEROTHERM
ACUREX Corporation

SECURITY CLASSIFICATION OF THIS PAGE (When Data Entered)

REPORT DOCUMENTATION PAGE

READ INSTRUCTIONS BEFORE COMPLETING FORM

1 REPORT NUMBER	2. GOVT ACCESSION NO. / 3. RECIPIENT'S CATALOG NUMBER
4 TITLE (and Subtitle)	5 TYPE OF REPORT & PERIOD COVERED
INVESTIGATION OF BOUNDARY LAYER RELAMINARIZATION ON A REENTRY VEHICLE NOSETIP	Final Report, September 20, 1974 — March 30, 1975
	6. PERFORMING ORG. REPORT NUMBER 75-145
7 AUTHOR(s)	8. CONTRACT OR GRANT NUMBER(s)
Calvin J. Wolf and Aemer D. Anderson	N60921-75-C-0052
9 PERFORMING ORGANIZATION NAME AND ADDRESS	10. PROGRAM ELEMENT, PROJECT, TASK AREA & WORK UNIT NUMBERS
Aerotherm Division/Acurex Corporation 485 Clyde Avenue Mountain View, California 94042	
11. CONTROLLING OFFICE NAME AND ADDRESS	12. REPORT DATE
Naval Ordnance Laboratory White Oak, Silver Spring, MD 20910	May 1975
	13. NUMBER OF PAGES 52
14 MONITORING AGENCY NAME & ADDRESS(if different from Controlling Office)	15. SECURITY CLASS. (of this report) Unclassified
	15a. DECLASSIFICATION/DOWNGRADING SCHEDULE

16. DISTRIBUTION STATEMENT (of this Report)

This document may only be distributed further by any holder with specific prior approval of Naval Ordnance Laboratory, White Oak, Silver Spring, Maryland

17 DISTRIBUTION STATEMENT (of the abstract entered in Block 20, if different from Report)

18 SUPPLEMENTARY NOTES

19 KEY WORDS (Continue on reverse side if necessary and identify by block number)

Relaminarization
Laminarization
Heat Transfer

20 ABSTRACT (Continue on reverse side if necessary and identify by block number)

A correlation for the distribution of heat transfer on a nosetip with a relaminarized boundary layer is developed and implemented in a general nosetip shape change code. A sensitivity study is made that shows that relaminarization results in significantly reduced heating rates in the sphere-cone tangent region of a reentry nosetip. This locally reduced heating is expected to have an impact, not as yet quantified, on the thermostructural performance of the nosetip.

DD FORM 1 JAN 73 1473 EDITION OF 1 NOV 65 IS OBSOLETE

UNCLASSIFIED

SECURITY CLASSIFICATION OF THIS PAGE (When Data Entered)

INVESTIGATION OF BOUNDARY LAYER RELAMINARIZATION ON A REENTRY VEHICLE NOSETIP

Calvin J. Wolf and Aemer D. Anderson

Aerotherm Division/Acurex Corporation
485 Clyde Avenue
Mountain View, California 94040

May 1975

Final Report, September 20, 1974 – March 30, 1975

Prepared for

NAVAL SURFACE WEAPONS COMMAND
White Oak Laboratory
Silver Spring, Maryland 20910

Contract No. N60921-75-C-0052

Under the
Naval Aeroballistics Renetry Technology
(ART) Program

TABLE OF CONTENTS

LIST OF ILLUSTRATIONS

LIST OF ILLUSTRATIONS (Concluded)

SECTION 1

INTRODUCTION

There is evidence that the boundary layer on a reentry nosetip can be turbulent in the neighborhood of the sonic point and laminar or "laminar-like" in a downstream region near the sphere-cone tangent point. This phenomenon is commonly called relaminarization or laminarization and results in locally reduced heat transfer rates. The major impact of this locally reduced heating is expected to be on the thermostructural performance of a nosetip. In order to evaluate the impact of this effect on nosetip performance, it is necessary to develop a method for predicting laminarization and evaluating the associated heat transfer distributions that is compatible with the codes used for nosetip design and performance studies. This methodology and a preliminary sensitivity study are the primary objectives of the present study.

Relaminarization has been observed in strongly accelerated axisymmetric and two-dimensional flows as well as in flows with convex streamwise curvature. Significant relaminarization and reductions in local heat transfer rate have been inferred from measured temperature distributions on calorimeter models tested in the Naval Ordnance Laboratory Tunnel No. 8 and on ATJ-S graphite nosetip models tested in the Air Force Materials Laboratory 50 MW arc. Since the phenomenon exists for such a wide range of conditions and configurations, it is necessary to delineate the parameters most relevant to nosetip laminarization. This choice is based on an analysis of the mechanics of nosetip boundary layers and on the need to develop a prediction scheme suitable for inclusion in the shape change codes used for design and performance studies.

Whereas it is anticipated that the major impact of relaminarization on nosetip performance is thermostructural, the scope of the present investigation is limited to the evaluation of the associated heat transfer distribution. This objective has been accomplished by the following steps

a. Review and evaluation of theoretical and experimental work on laminarization

b. Development and incorporation into a design code of a relaminarization heat transfer correlation

c. Sensitivity study to determine the effects of trajectory and nose radius variation.

The results of the sensitivity study indicate significantly reduced heating rates near the sphere-cone tangent point of a nosetip and indicate a need for further work in order to determine the full extent of the thermostructural ramifications.

Section 2 of this report highlights some of the important aspects of the literature review and evaluation published separately (Wolf and Anderson, Reference 1), Section 3 documents the methods and results of the correlation development task, and Section 4 details the results and conclusions of the sensitivity study. Primary conclusions are presented in Section 5.

SECTION 2

LITERATURE SURVEY

The objective of this phase of the investigation was to assemble and evaluate available information on the phenomenon of relaminarization. The detailed results of this critical survey are reported by Wolf and Anderson (Reference 1).

Since what were probably the first observations of laminarization by Sternberg in 1954 (Reference 2), a large number of theoretical and experimental studies have been devoted to the subject. These references were evaluated in terms of the need to implement the results in the shape change codes used for nosetip design. Hence, the choice of variables is limited to the boundary layer parameters that appear in the von Karman integral momentum equation.

Known laminarizing flows can be broadly classified into two groups, which are:

a. Boundary layers subjected to large streamwise accelerations

b. Boundary layers subjected to large normal accelerations.

Of these two groups, (a) has been the most widely studied. Experimental data covering a wide range of pressure gradients, initial Reynolds numbers, configurations and heat and mass transfer rates are available. Some of the data are very detailed, including measurements of the structure of the turbulence and the intermittency of a laminarizing boundary layer. In contrast, there is relatively less data on boundary layers which laminarize as a result of large normal accelerations. In this case there are only a few reported studies and the experiments are less detailed. This information is summarized on Figure 4 of Reference 1, which is a tabulation of experimental sources and the parameters that were measured.

A similar situation exists with respect to theoretical descriptions of laminarizing flows. The theories, (see Wolf and Anderson, Reference 1) range from methods based on modifications of the usual approach to the integral momentum equation to multi-equation turbulence models. Some of the theories include compressibility and streamwise curvature as well as the necessary extensions for the prediction of heat transfer. Following the submittal of Reference 1, several recent additional contributions by Narasimha and Sreenivasan (Reference 3), Baker and Launder (References 4 and

5), and Deissler (References 6 and 7) were examined. However, the main conclusion of Wolf and Anderson (Reference 1) must remain as stated, namely, that there is no really reliable and well tested method for predicting laminarizing flows. Even if it is judged that one (or more) of the existing theories shows satisfactory comparison with a certain subset of the data, it is extremely unlikely to be applicable to a hypersonic nosetip. Furthermore, the kind of correlation that would be of use for practical design calculations was unavailable.

A large number of different parameters for characterizing relaminarization have been suggested. Wolf and Anderson (Reference 1) evaluated these with respect to the needs of the present study. Their conclusions are based mostly on the fact that only relatively simple integral and edge variables are available from the current design codes, but also on the lack of definitive evidence for the validity of any one of the proposed parameter(s).

SECTION 3

CORRELATION DEVELOPMENT

It is immediately apparent that a nosetip environment contains both of the factors known to cause laminarization of other flows, i.e., streamwise and normal acceleration. In addition, a nosetip boundary layer is influenced by the complications of large surface roughness, compressibility and surface mass transfer. Therefore, it is necessary to identify the dominant nosetip laminarization mechanism as a preliminary step in developing a correlation. The approach to this task is to examine separately each class of known laminarizing flows and on the basis of these results construct a correlation for a nosetip boundary layer.

There are four relatively recent experimental studies of plane boundary layers with streamwise acceleration that contain suitably detailed information on integral boundary layer parameters: Blackwelder and Kovasznay (Reference 8), Patel and Head (Reference 9), Badri Narayanan and Ramjee (Reference 10), and Jones and Launder (Reference 11). The data from these experiments were examined in detail, and the methods and results are given in Section 3.1 below. The effort to correlate these data is only partially successful due to what are believed to be inconsistencies in the data. However, sufficient qualitative information was obtained to justify the use of a correlation based on other data, as described in Section 3.2.

3.1 DATA REDUCTION AND CONSISTENCY ANALYSIS

In order to facilitate the necessary analysis, the data were transferred to punched cards and a code was written to test various aspects of the data and for use as a tool in correlation development. Input to the code are the measured distributions of all the variables in the integral momentum equation

$$\frac{1}{Re_{\delta^*}} \frac{dRe_{\delta^*}}{ds} + (H + 1) Re_{\delta^*} K = C_f/2$$

where s = streamwise coordinate

u_e = boundary layer edge velocity

δ^* = displacement thickness

θ = momentum thickness

τ_w = wall shear stress

ρ_e = edge mass density

ν_e = edge kinematic viscosity

and Re = u_e/ν_e = unit edge Reynolds number

Re_θ = $u_e\theta/\nu_e$ = momentum thickness Reynolds number

H = δ^*/θ = shape factor

K = $\nu_e/u_e^2\ du_e/ds$ = pressure gradient parameter

C_f = $2\tau_w/(\rho_e u_e^2)$ = skin friction coefficient

One basic section in the code generates a cubic spline fit to any variable with a controllable amount of smoothing using a least squares criterion. The method is an adaption of that due to Reinsch (Reference 12) and is necessary in order to obtain accurate interpolation between data points and to calculate well behaved derivatives of the data where needed. An example of the results of using this routine is shown in Figure 1 where a fit to the measured edge velocity, ($U_e(s)$), is compared to the data. Figure 2 shows the corresponding distribution of K(s), calculated from the smoothed cubic spline and compared to that given by Blackwelder and Kovasznay (Reference 8). It is seen that the method gives good results, both in terms of the fit to the data and for calculating derivatives. The differences between the curves and the data indicated by Figures 1 and 2 are not significant in terms of the effect on the subsequent analysis or in terms of evaluating the method. Instead, the "goodness of fit" is dependent on control inputs to the program, which, when appropriately chosen, will generate cubic splines that pass exactly through the data. An example, of very little smoothing is given in Figure 3, which shows the shape factor distribution for the data of Blackwelder and Kovasznay (Reference 8) and its analytic representation.

Another section of the code contains the logic and subroutines necessary for using the data to solve the integral momentum equation. For example, with Re, C_f and $Re_\theta(0)$ taken from the data, one option calculates $Re_\theta(s)$ by integration of the differential equation using a fourth order Runge-Kutta scheme. Another option used fits to the measured distributions of Re, H and $Re_\theta(s)$ to calculate $C_f(s)$. The code also facilitates the prediction of boundary layer development when, as is the case here, the initial and freestream conditions are known and when a correlation that specifies a relationship between Re_θ, C_f and H is postulated.

The results of the analysis of the data and various correlations are given in the next sections, wherein first a special case and then the general case of streamwise accelerated boundary layers are considered.

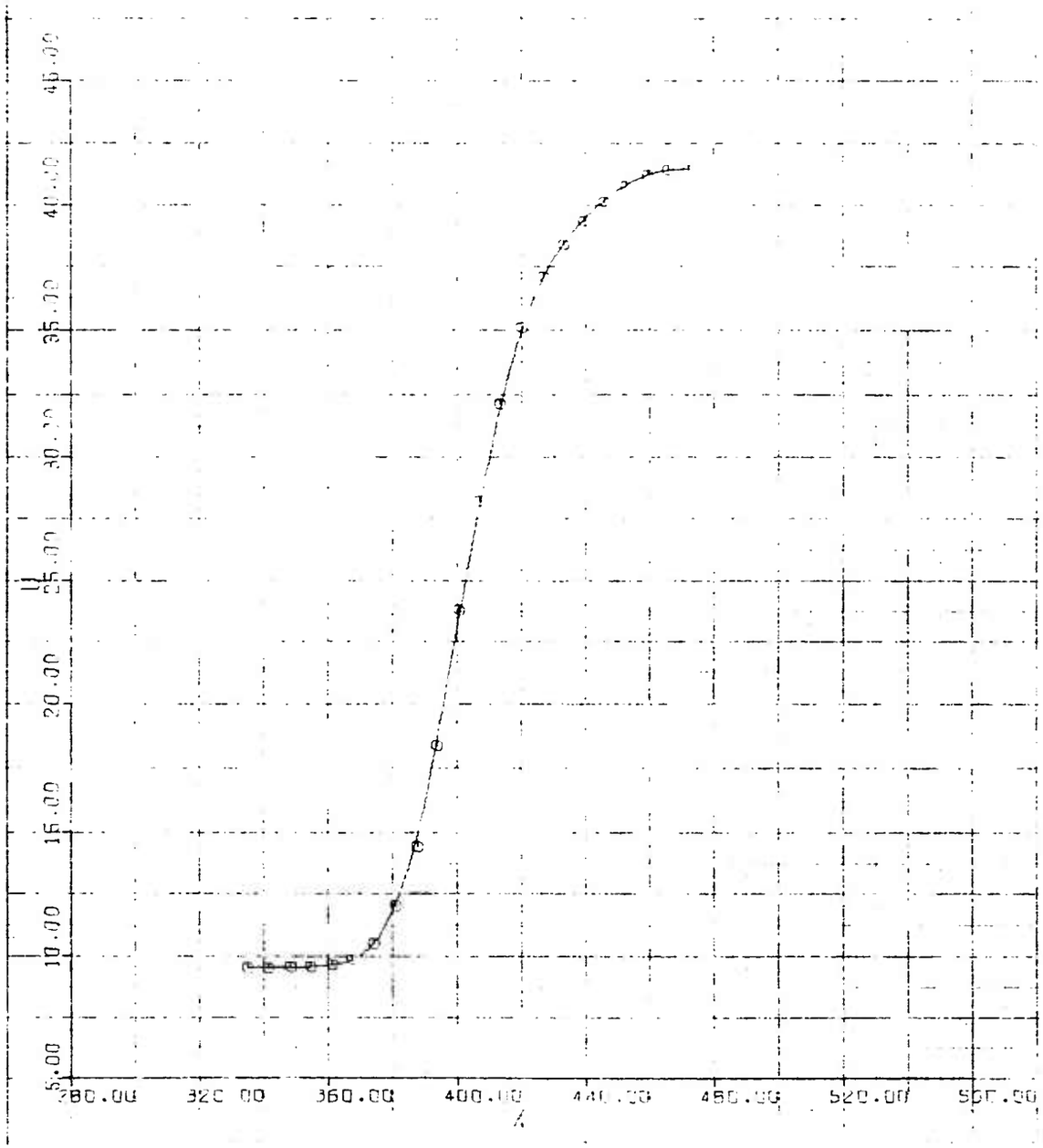

Figure 1. Comparison of the measured edge velocity data of Blackwelder and Kovasznay (Reference 8) with the smoothed cubic spline fit.

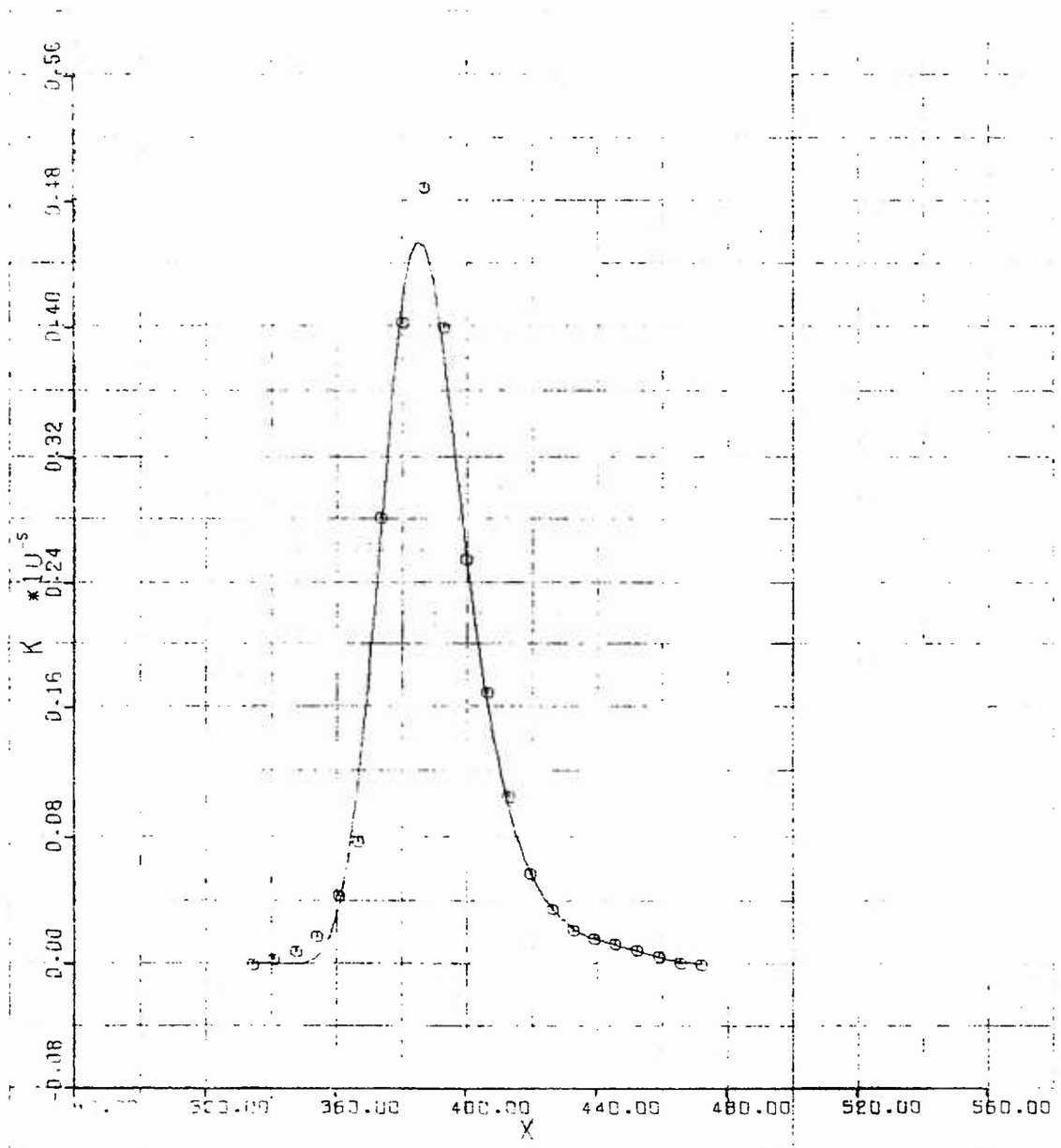

Figure 2. Comparison between the pressure gradient parameter calculated by Blackwelder and Kovasznay (Reference 8) and calculated from spline fit.

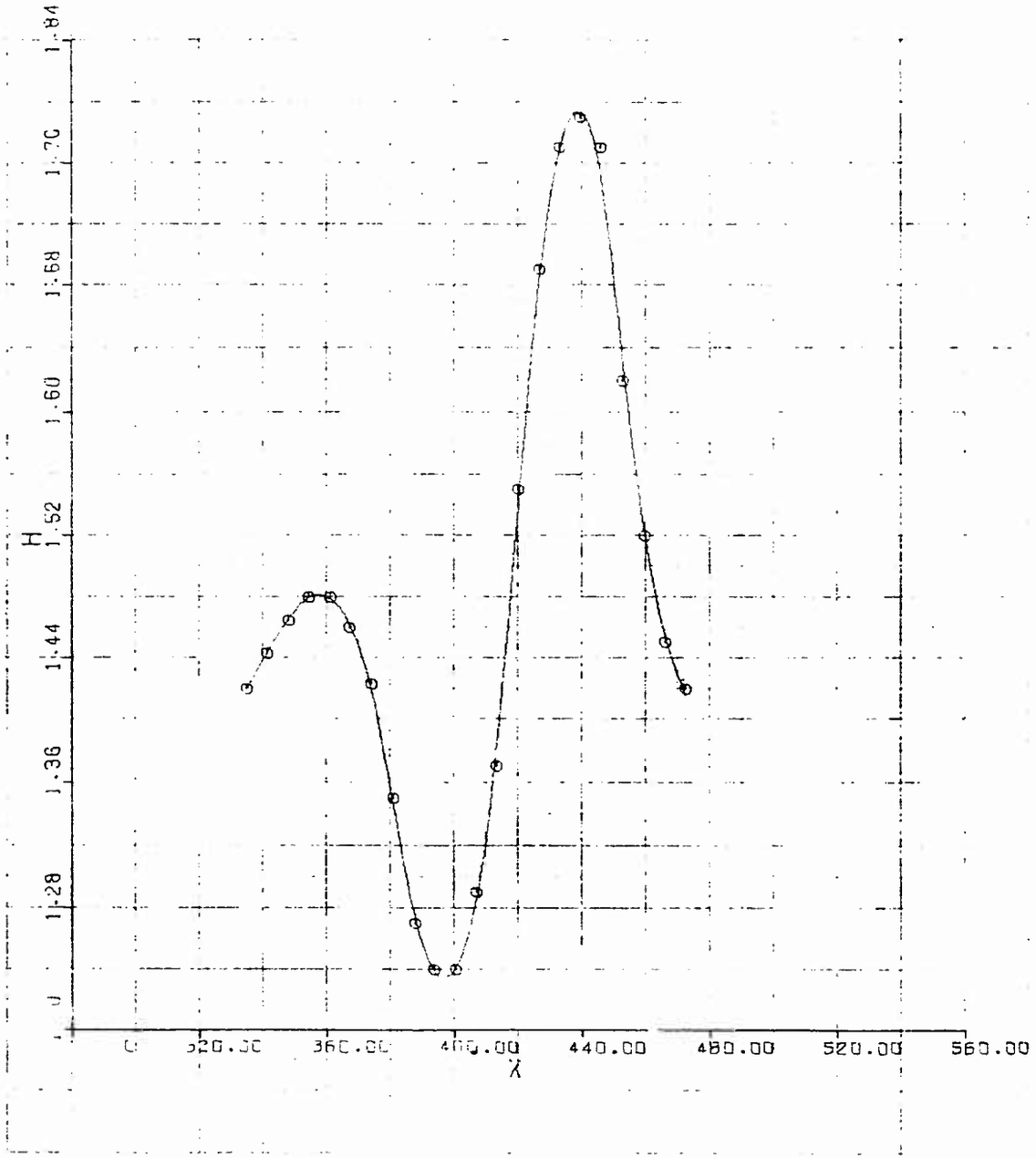

Figure 3. Comparison of the shape factor distribution measured by Blackwelder and Kovasznay (Reference 8) with the smoothed cubic spline fit.

3.1.1 Equilibrium Sink Flows

An equilibrium sink flow is a boundary layer for which the pressure gradient parameter,

$$K = \frac{\nu}{u_e^2} \frac{du_e}{ds} = \text{constant}$$

This condition is obtained experimentally from the flow between convergent plane walls. Its significance is that is describes the asymptotic behavior of an accelerated boundary layer (after relaxation effects) subject to constant K. Therefore, an equilibrium sink flow represents a limiting state for an accelerated turbulent boundary layer.

For this circumstance, it has been shown theoretically and experimentally by Launder and Jones (Reference 13), and Jones and Launder (Reference 11) that K is the single independent parameter that characterizes the flow. A correlation based on these studies was developed and tested against theory and experiment with satisfactory results. This correlation is given by the following expressions:

$$\left.\begin{aligned} Re_{\theta T} &= 0.0117\ K^{-0.832} \\ H_T &= H_o\sqrt{1 + K/K_R} \end{aligned}\right\} \text{Turbulent ; } K \leq K_T$$

$$\left.\begin{aligned} Re_{\theta L} &= 0.3762\ K^{-0.5} \\ H_L &= 2.069 \end{aligned}\right\} \text{Laminar ; } K \geq K_L$$

$$\left.\begin{aligned} Re_\theta &= (1 - W)\ Re_{\theta T} + WRe_{\theta L} \\ H &= (1 - W)\ H_T + WH_L \\ W &= (1 - \cos \pi Z)/2 \\ Z &= \frac{\log K - \log K_T}{\log K_L - \log K_T} \end{aligned}\right\} \text{Laminar-Turbulent ; } K_T < K < K_L$$

The parameters chosen for this correlation are:

$K_T = 0.68\ (10^{-6})$

$K_L = 8.0\ (10^{-6})$

$K_R = 8.0\ (10^{-6})$

H_0 = 1.2 to 1.5

where H_0 is the experimental shape factor at the upstream position where K = 0.

This correlation is a composite of existing theoretical and experimental results. When $K > K_L$ it gives results identical to the known exact (analytical) solution for a laminar sink flow (see Schlichting, Reference 14) For $K < K_T$, it matches the results of the calculations, based on a mixing length model, of Launder and Jones (Reference 13). When $K_T < K < K_L$, the given form of the weighting factor, W, interpolates between the turbulent and laminar extremes with an analytical form that matches the slopes of the extremes at the limit points.

When K is specified, H and Re_θ are determined by the above correlation, and the skin friction coefficient is found from the integral momentum equation

$$C_f = 2(H + 1)\, Re_\theta K$$

which is the appropriate form when $dRe_\theta/dx = 0$.

Results obtained from the correlation and representative data are shown in Figures 4, 5 and 6. It is seen that the trend and the magnitude of the data are correctly given by the correlation.

Therefore, a simple computational scheme has been established for determining the asymptotic state (and integral properties) of an initially turbulent boundary layer when the imposed pressure gradient is such as to make K = constant. This correlation does not describe the process of evolution to the asymptotic state but it is useful for estimating the magnitude of the pressure gradient necessary to eventually obtain a given degree of laminarization. Thus, Figure 4 shows that the often quoted value of $K = 3(10^{-6})$ corresponds to an asymptotic state that is about "half laminar" and "half turbulent". Furthermore, the summary of experimental and theoretical results represented by the correlation shows that laminarization is a process that occurs to varying degrees over a range of pressure gradients given by $0.7\ (10^{-6}) < K < 8\ (10^{-6})$.

These results provide useful guidelines for identifying many qualitative features of other experimental circumstances, and in particular are good indicators of nonequilibrium effects.

3.1.2 Nonequilibrium Plane Flows

A turbulent boundary layer responds to changes in edge conditions by processes that require finite time. When conditions are such that a boundary layer is continuously adjusting to changes in external pressure gradient, it is nonequilibrium if the rate of adjustment is slower than the rate at which conditions change. In terms of the parameter K, a measure of the rate of change of external conditions is

A-10903

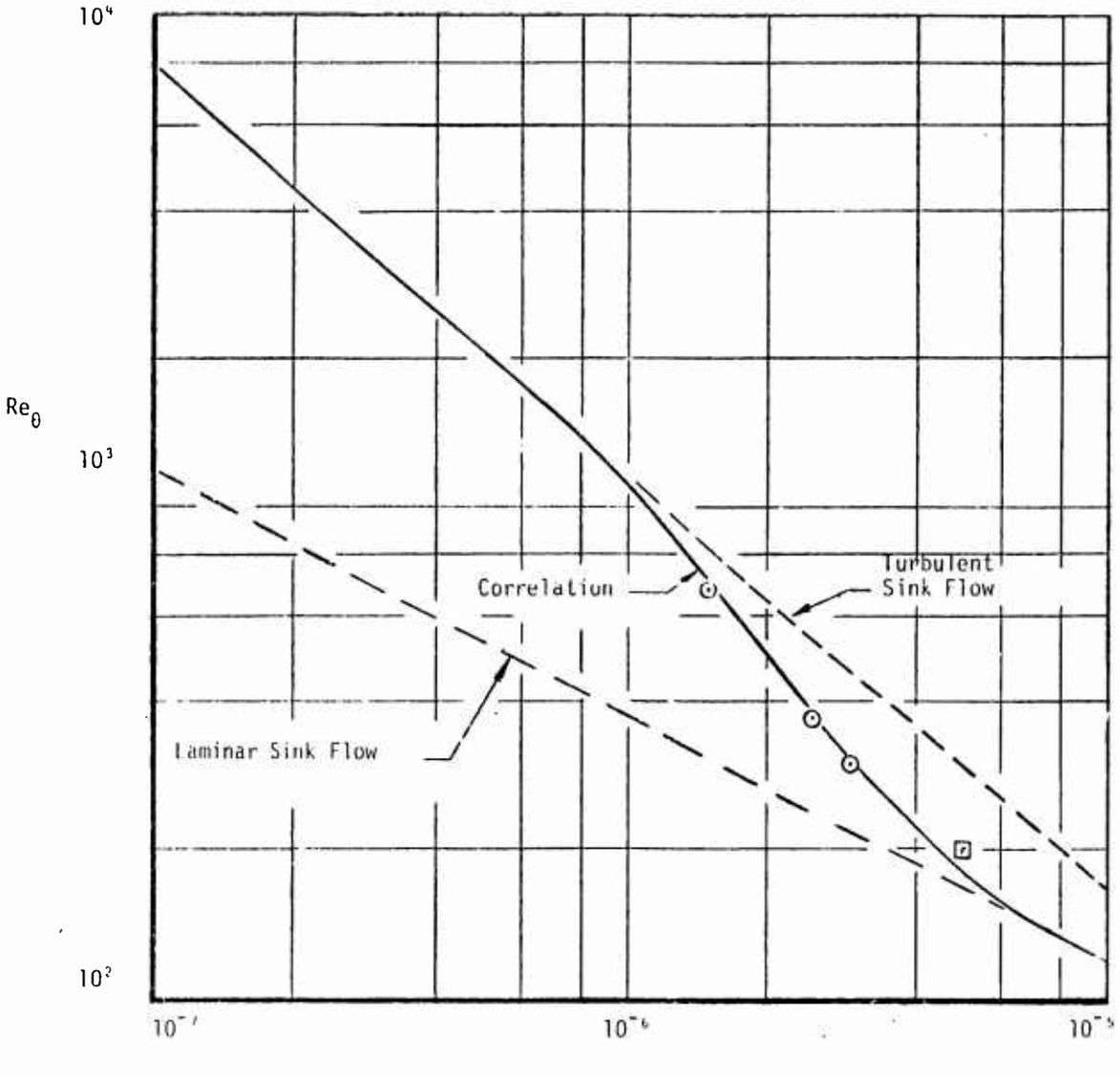

Figure 4. Sink flow correlation for Re_θ; data from References 10 (⊡) and 11 (⊙).

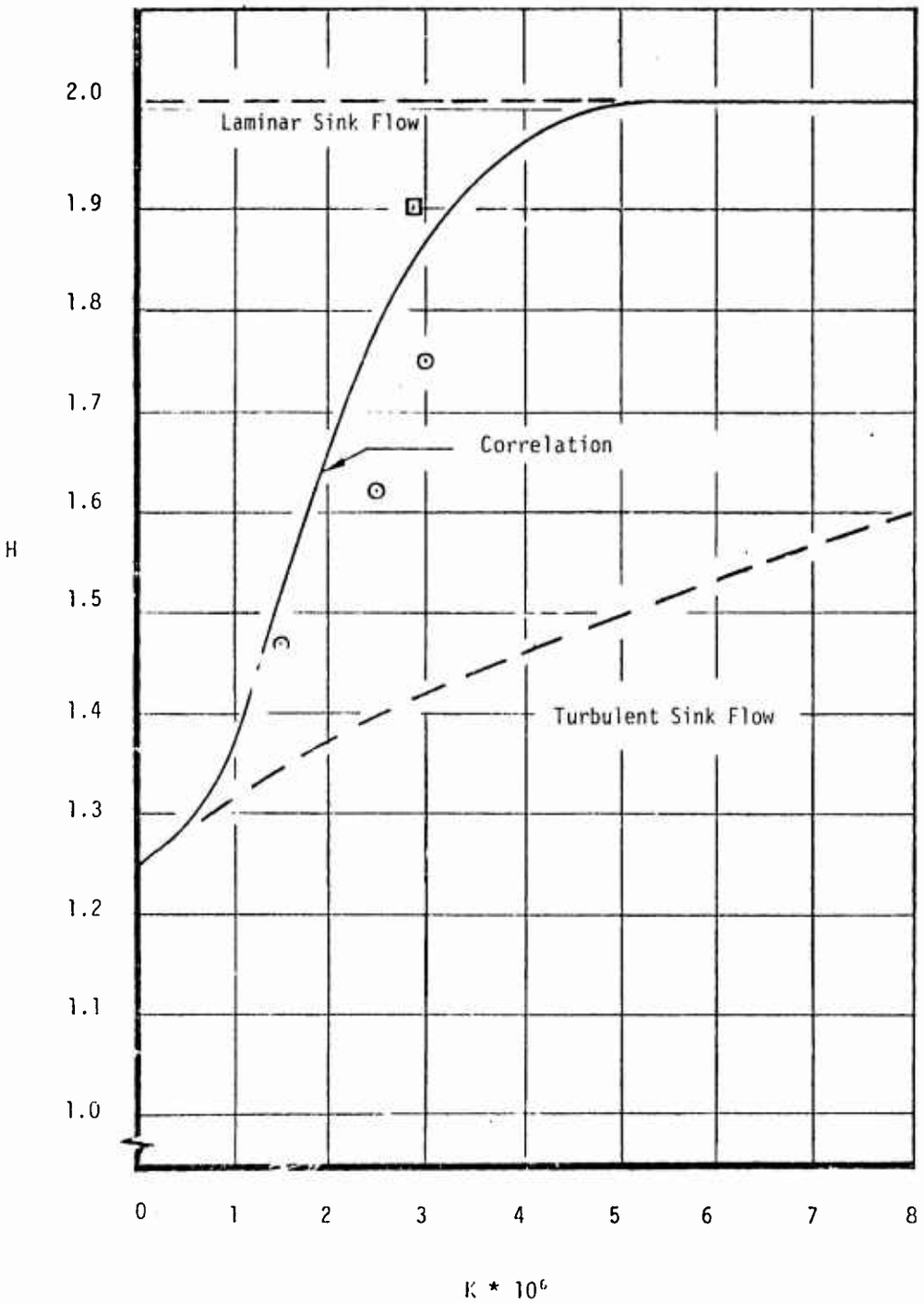

Figure 5. Sink flow correlation for H; data from References 10 and 11.

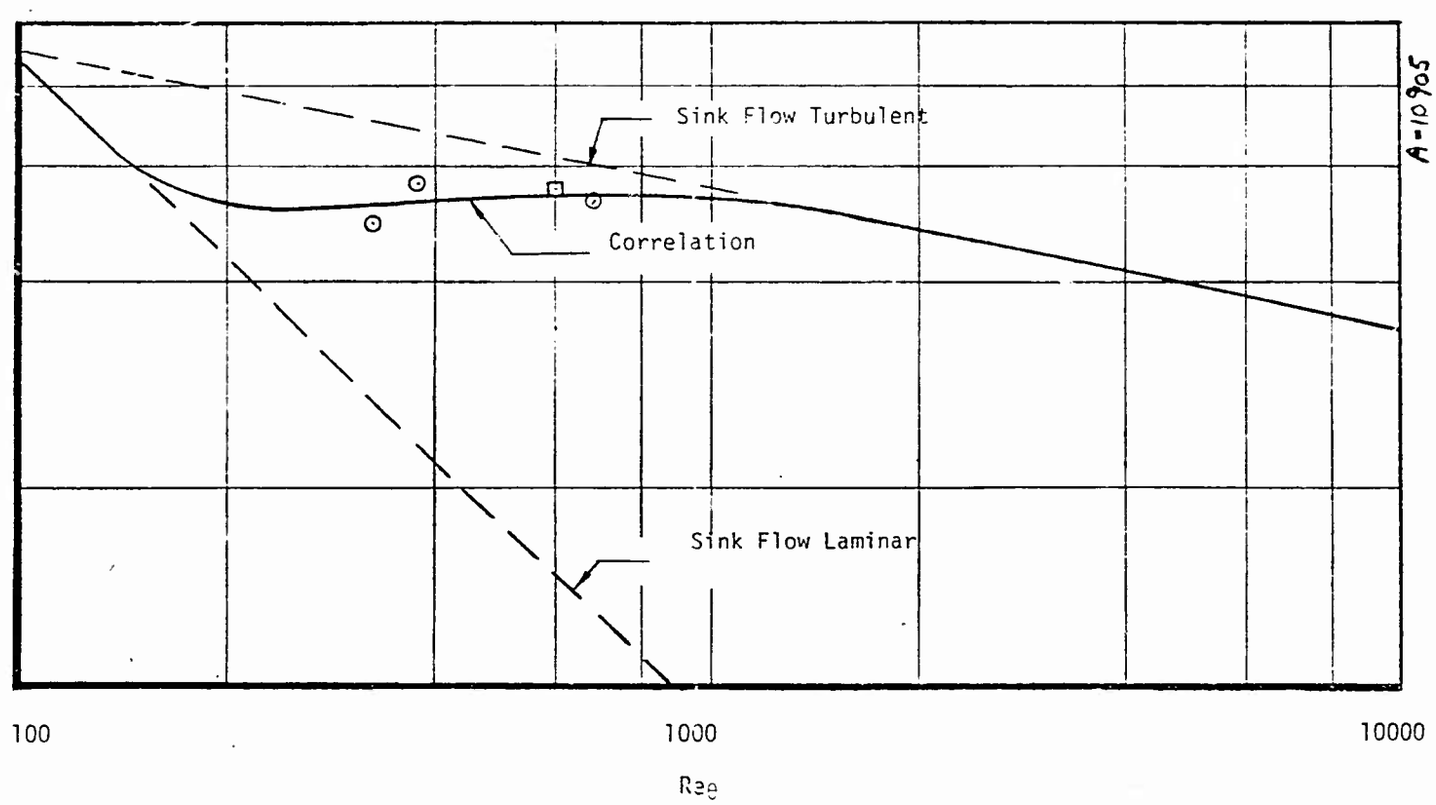

Figure 6. Comparison of skin friction coefficient results using sink flow correlations; data of References 10 and 11.

$$\frac{1}{\tau_s} = u_e \frac{dK}{ds} = \frac{DK}{Dt}$$

where τ_s is the time scale over which eage conditions change. If τ_e is taken as representative of the time required for a boundary layer to react to changing conditions (i.e., to achieve equilibrium), then it follows that

$$\tau_e > \tau_s$$

for a typical nonequilibrium laminarizing flow. This observation is derived from the qualitative features of the data and is also the basic hypothesis of the recent theory of Deissler (Reference 6).

It is obvious that τ_e is a complex function of the turbulent velocity field in a boundary layer. In fact, it represents the sum total of the dynamical self-interactions between turbulent components as well as coupling with the mean velocity field. A theoretical prediction of τ_e would require the solution of a complex set of partial differential equations, which is a task that is the subject of current basic research and obviously beyond the scope of design calculations

Nevertheless, correlation of the low speed data must in some way account for nonequilibrium effects. This is shown by an application of classical correlations to the experimental conditions. For these test cases, the correlations given by White (Reference 15) were chosen, which are

$$C_f = \frac{0.3e^{-1.33H}}{(\log Re_\theta)^{1.74+0.31H}}$$

$$\beta = \frac{\delta^*}{\tau_w}\frac{dp}{dx} = -\frac{2}{C_f} H Re_\theta K$$

$$P = 0.8(0.5 + \beta)^{3/4}$$

$$A = \frac{2 + 3.179P + 1.5P^2}{0.41(1 + P)}$$

$$H = \frac{\sqrt{2/C_f}}{\sqrt{2/C_f} - A}$$

These correlations are the result of a large amount of carefully scrutinized data as well as theoretical considerations. They represent a composite of the work

of Ludwig and Tillmann (Reference 16), Coles (Reference 17) and others. Basic elements in the construction of these expressions are the "law of the wall" and the "law of the wake", which are described by White (Reference 15) and widely known. It should be noted that these are usually regarded as valid for equilibrium boundary layers only, i.e.,

$$\tau_e \geq \tau_s$$

and are sometimes referred to as "equilibrium correlations". As such, the usual application of these equations never encounters the circumstances where

$$n < \frac{1}{2}$$

which, for the large K of a laminarizing flow, is very common and results in an imaginary value of P. Taking into account the fact that the parameter P has its origin in the "law of the wake", P has been set equal to zero for any $n < 1/2$, consistent with the theory of Deissler (Reference 6) and with the inference from experimental velocity profiles that the wake component disappears with large pressure gradient.

Typical results of integration of the integral momentum equation using these correlations are shown in Figure 7. The initial conditions for the integrations ($Re_\theta(o)$) were taken from the data, as were the distributions of edge velocity. Also shown on Figure 7 are the data, which are seen to compare very poorly with the predictions. The data show a streamwise development of Re_θ different from the predictions and, more importantly, a very different trend for $C_f(s)$. If a boundary layer is considered to have laminarized at that streamwise position where Re_θ and C_f attain values equal to those given by a laminar prediction (no other definition is possible with integral parameters), then Figure 7 shows that the equilibrium correlations fail to predict "laminarization". Further examination of the data shows that the streamwise position where laminarization occurs is downstream of the point where K is a maximum This is a manifestation of nonequilibrium effects, and can be characterized as a "delay".

In qualitative terms, some of the data show a very pronounced delay and some do not while other data indicate a possible approach to turbulent sink flow behavior which the data of Blackwelder and Kovasznay (Reference 8) lack. Therefore, it is necessary to identify the reasons for these apparently different modes of laminarization and to identify a parameter that correlates these effects.

As a preliminary part of this task and as a more or less routine check on the data and the code used for its analysis, the measured distributions of Re, H, K and C_f were examined for consistency with respect to the integral momentum equation. The

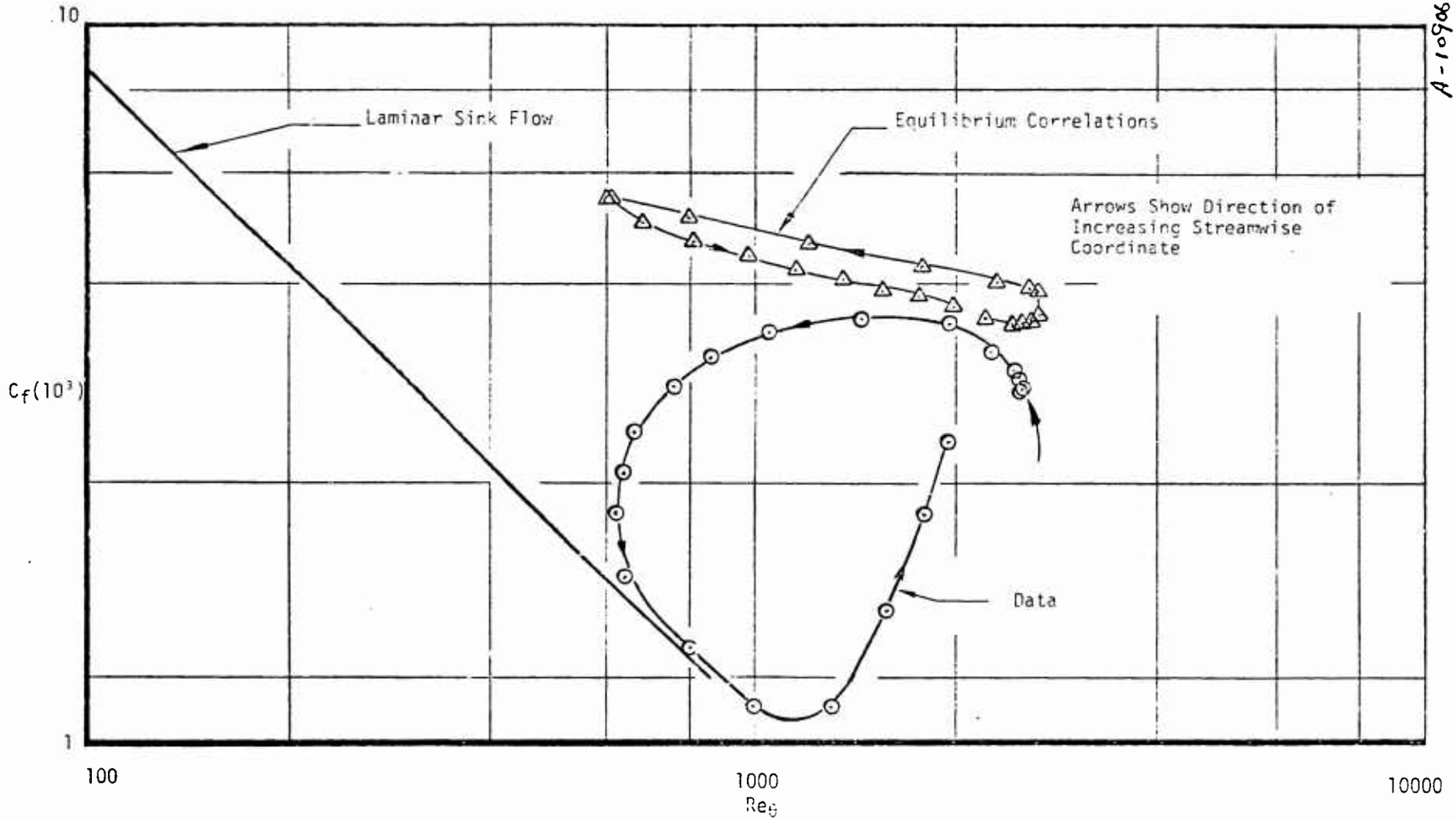

Figure 7. Equilibrium correlations compared to data of Blackwelder and Kovasznay (Reference 8).

method of using smoothed cubic spline fits and Runge-Kutta integration, previously described, was used. The results are, that generally, the measured and calculated distributions of Re_{θ} have the same trends but differ significantly in magnitude as shown in Figures 8, 9 and 10. Using the subscripts m and c to denote measured and calculated, respectively, a convenient measure of the discrepancy is the quantity

$$(Re_{\theta m} - Re_{\theta c})/Re_{\theta m}$$

An annotated summary of the discrepancies in terms of the above parameter for each data set is as follows:

A. Blackwelder, et al. (Reference 8)

- 10 percent discrepancy in region of maximum laminarization
- 50 percent discrepancy in retransition region

B. Patel, et al. (Reference 9)

- -95 percent discrepancy in region of maximum laminarization
- Noticeably different trend in approach to miminum Re_{θ}

C. Badri Narayanan, et al. (Reference 10)

- -53 percent, -60 percent, -90 percent (worst case) increasing with initial Re_{θ}
- Better agreement is found when smoothing is applied to u_e and K is recalculated

Additional understanding of the inconsistencies in the data comes from reversing the procedure. That is, compute dRe_{θ}/dx from a smoothed cubic spline fit to the measured Re_{θ} distributions, use measured H and Re distributions and calculate C_f from the integral momentum equation. This procedure gives C_f from 0.1 to 12 times the measured values. In some case, for certain regions, calculated C_f is negative, which is a physical impossibility.

A number of cross checks of the code and the method of analysis were made. It was shown, for example, that smoothing of the measured edge velocity distributions results in pressure gradient, (K), distributions slightly different than those calculated by the authors of the experimental studies. However, such differences are insufficient to account for the overall lack of comparison. Another test case was the calculation of a flat plate boundary layer and a separate test on the integration subroutine that compared the numerical solution to a known exact solution. In all cases the code and the numerical methods were found to be correct.

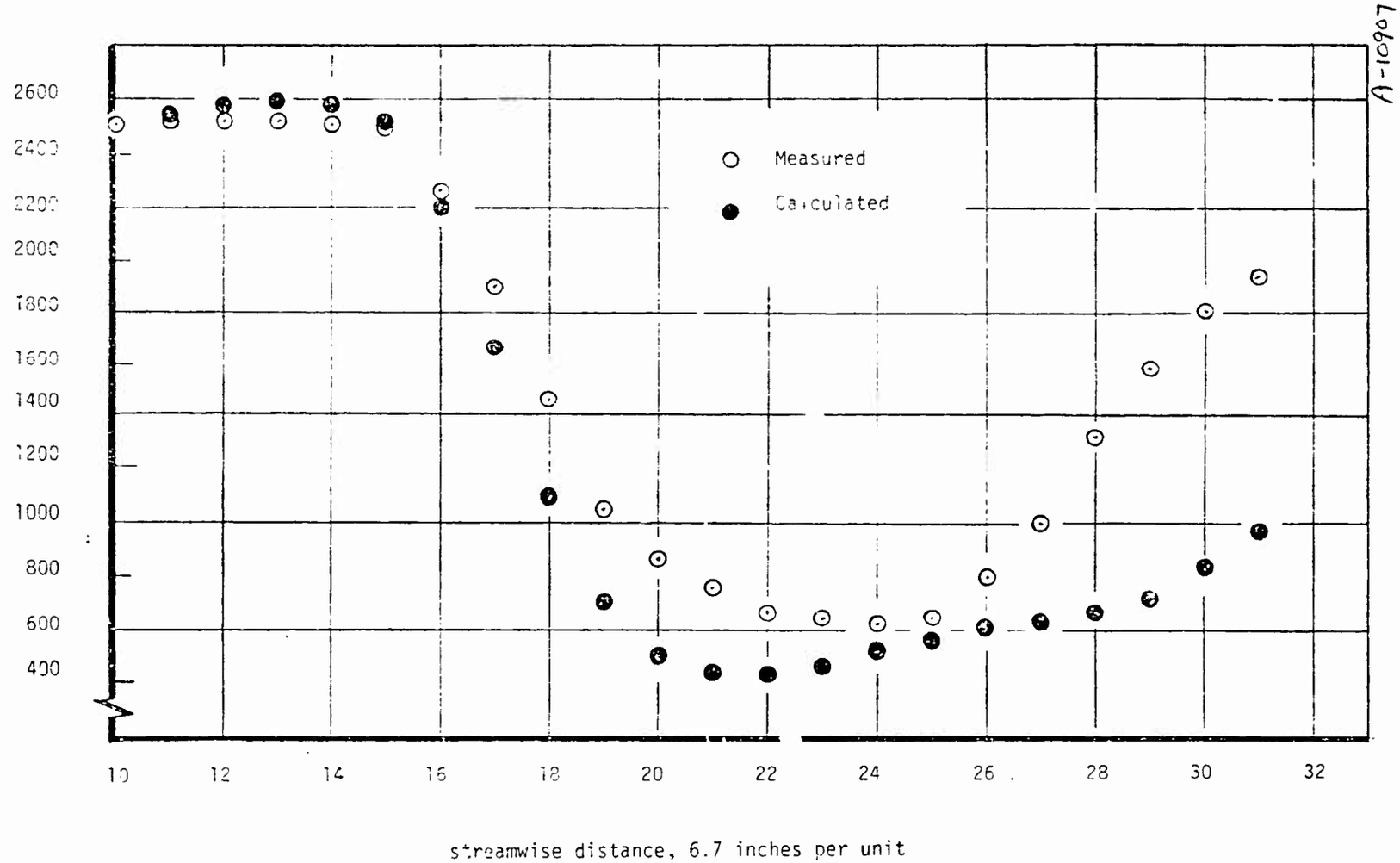

Figure 8. Calculated and measured Re_θ distributions for the data of Blackwelder and Kovasznay (Reference 8).

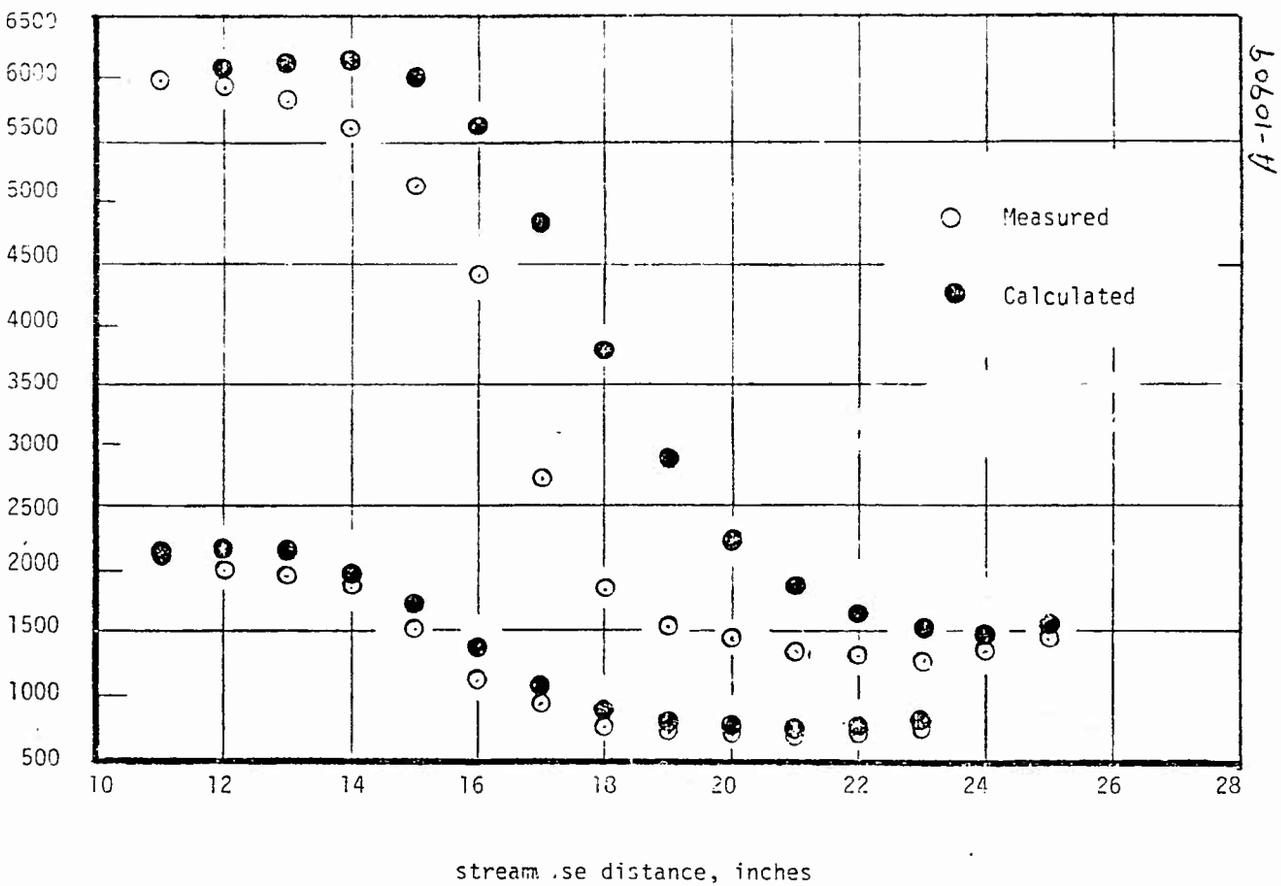

Figure 9. Calculated and measured Re_θ distributions for the data of Patel and Head (Reference 9).

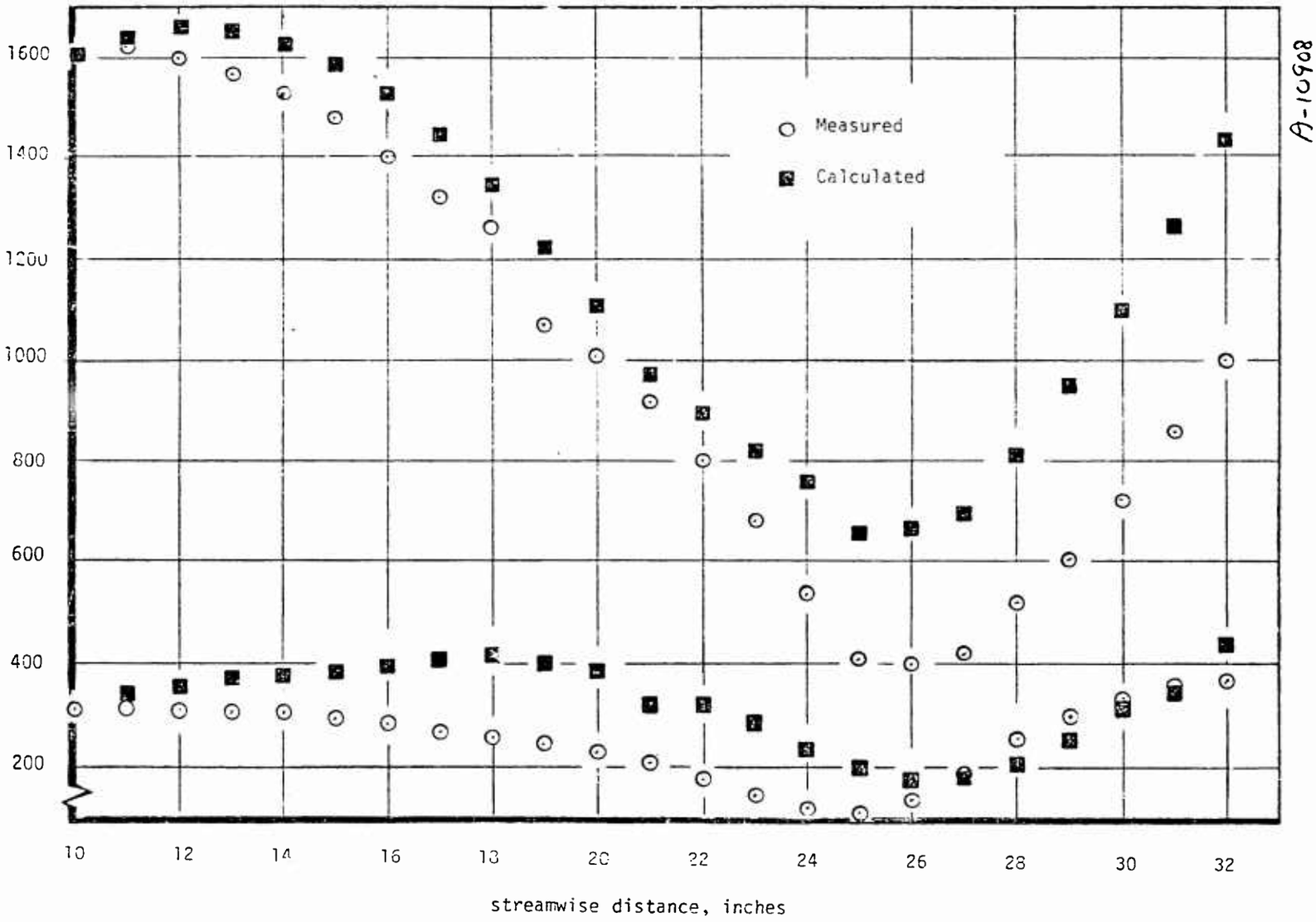

A-10908

Figure 10. Calculated and measured Re_θ distributions for the data of Padri Narayanan and Ramjee (Reference 10).

A further inquiry examined the question of whether or not the integral momentum equation is valid for a strongly accelerated flow. The only aspect of this question that needs to be addressed concerns the boundary layer equations themselves, because the von Karman equation is just an integrated form of these equations. The usual boundary layer approximation of the Navier-Stokes equations neglects a term in the streamwise momentum equation, i.e., it is assumed that

$$\frac{\partial^2 u}{\partial s^2} << \frac{\partial^2 u}{\partial n^2}$$

where n is normal to the wall.

This inequality was examined for the case of the present circumstances and found to be satisfied; the neglected term is indeed several orders of magnitude smaller. No evidence supporting the need for the full Navier-Stokes equations has been found.

With regard to the experiments, there are a number of well known grounds on which to question the validity of data of this kind. In the present case, it is appropriate to note these:

a. The shape of the mean velocity profile is more than usually difficult to measure accurately

b. Wall shear stress measurements by ordinary methods are questionable

c. The mean flow may not be two-dimensional.

It is not clear which one or more of the above factors is most relevant to each of the experiments considered. One of the authors (Blackwelder, Reference 18) has reported that there were initial doubts about the two-dimensionality of the flow but that the apparatus was corrected. The data from this and another experiment were tested against the theory of Deissler (Reference 19) and it was reported by Deissler (Reference 19) that the wall shear stress measurements of Blackwelder and Kovasznay (Reference 8) did not compare as well as did those of Patel and Head (Reference 9).

Overall it seems fair to judge that there are serious fundamental questions about the data that are presently unanswerable. Under these conditions, it is only possible to get semi-quantitative information about the trend of the data and to make as much use of this as possible.

3.2 LAMINARIZATION ON NOSETIP CONFIGURATIONS

From the results of the previous sections, it is evident that a definitive delineation of the mechanism of nosetip laminarization is not yet available. However, it is shown below, that a combination of an empirical expression and some

reasonable arguments leads to a useful correlation for the prediction of nosetip laminarization in design studies. The arguments are partly intuitive but also based on known theoretical and experimental results for flows with normal acceleration (streamwise curvature). This correlation is described in the following, starting with its empirical basis and showing the results of test cases at the end of the section.

3.2.1 The Correlation

The degree of laminarization at the tangent point of a sphere-cone was shown by Anderson and Jackson (Reference 20) to be well correlated by conditions at the sonic point. When the degree of laminarization is defined as

$$\gamma = \frac{q_T - q}{q_T - q_L}$$

where q is heat flux and the subscripts T and L refer to turbulent and laminar respectively, it was shown that

$$\gamma_{\text{fore cone}} = 1.7(10^6)\lambda^{-3/2}$$

where

$$\lambda = \left(\frac{T_0}{T_w}\right)^{2/3} \frac{u_e^* k^{4/9} R_c^{*5/9}}{\nu_e^*}$$

in which T_w/T_0 is the wall temperature ratio, u is the streamwise velocity, k is the surface roughness height, R_c is the streamwise radius of curvature, ν is the kinematic viscosity, e refers to the edge of the boundary layer, and * refers to the sonic point. The correlation and the data are shown on Figure 11.

The data base for this correlation includes data from the rough wall calorimeter experiments of the PANT program (Series A and J) and those from the NOL ART tests (Series 3 and 4). These data cover a fairly wide range of nose radius, surface roughness, unit Reynolds number, wall temperature ratio and geometry.

The needs of the current study are met by establishing a procedure for calculating the distribution of γ from an appropriate point upstream to the cone-tangent point where $\gamma_{F.C.}$ is known. There are two main considerations to be taken into account in this process. The first is the choice of variables and the second is the determination of an analytical form.

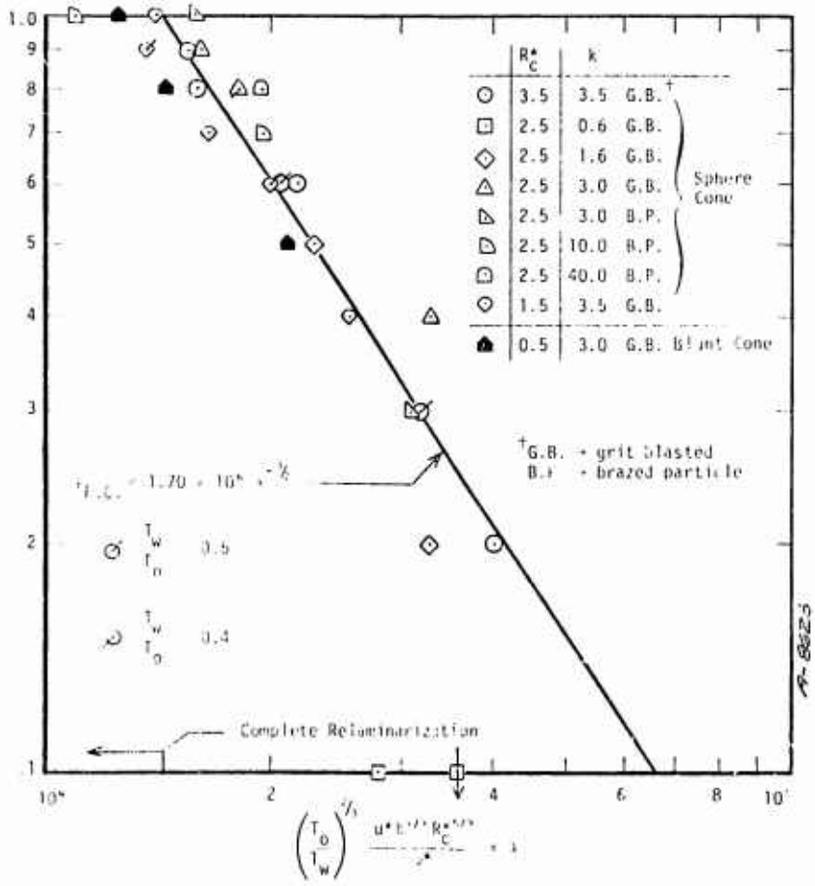

Figure 11. Comparison of fore cone relaminarization correlation and wind tunnel data.

With regard to the choice of variables, it is noted that on a nosetip, the pressure gradient parameter

$$K = \frac{\nu_e}{u_e^2} \frac{du_e}{ds}$$

is infinite at the forward stagnation point and decreases monotonically with s, except for a region somewhat downstream of the sonic point, where it reaches a small relative maximum. A typical distribution is shown in Fig. 12, along with the calculated laminar and turbulent and the measured heat transfer distributions for one of the PANT Series J tests (Run 602).

The point to be noted is that in the region of laminarization on a nosetip, K is always much less (by a factor of approximately 10) than it is at the location of transition. In contrast, the plane flow data (with streamwise pressure gradient) of Blackwelder and Kovasznay (Reference 8) and others show, at least qualitatively, that laminarization downstream of a point where a given turbulent condition exists is the result of an increase of K with streamwise distance. Thus, it seems unlikely that nosetip laminarization is strongly influenced by the streamwise pressure gradient.

The other aspect of the comparison of the effect of streamwise pressure gradient in low speed flows with the case of a nosetip is the magnitude of K. Figure 12 is representative of the circumstances on a nosetip, and shows that $K > 3(10^6)$ over most of the sphere ($S/R_N < 1.2$). This is large enough to cause laminarization according to the usual low speed criterion for smooth walls. However, the effect of roughness on low speed laminarization is not known (either experimentally or theoretically). It is intuitively reasonable that the value of K necessary for laminarization increases with increasing roughness. Hence, it is argued that roughness is a major factor in determining the state of a boundary layer on a nosetip and accounts for the differences between the magnitude of K on a nosetip and in a low speed flow at points where the degree of laminarization is similar.

The remaining variable in the fore-cone correlation is the streamwise radius of curvature, R_c, and it follows that the extension of $F_{F.C.}$ should involve a variable associated with this effect. The work of Prandtl (Reference 21), Rotta (Reference 22), and Thomann (Reference 23) supports the contention that the main effect of streamwise curvature is to establish a pressure gradient normal to the surface, which inhibits turbulent mixing. The magnitude of the normal pressure gradient is conveniently measured by

$$\frac{\rho_e u_e^2}{R_c}$$

which typically has a distribution on a nosetip as shown in Figure 12.

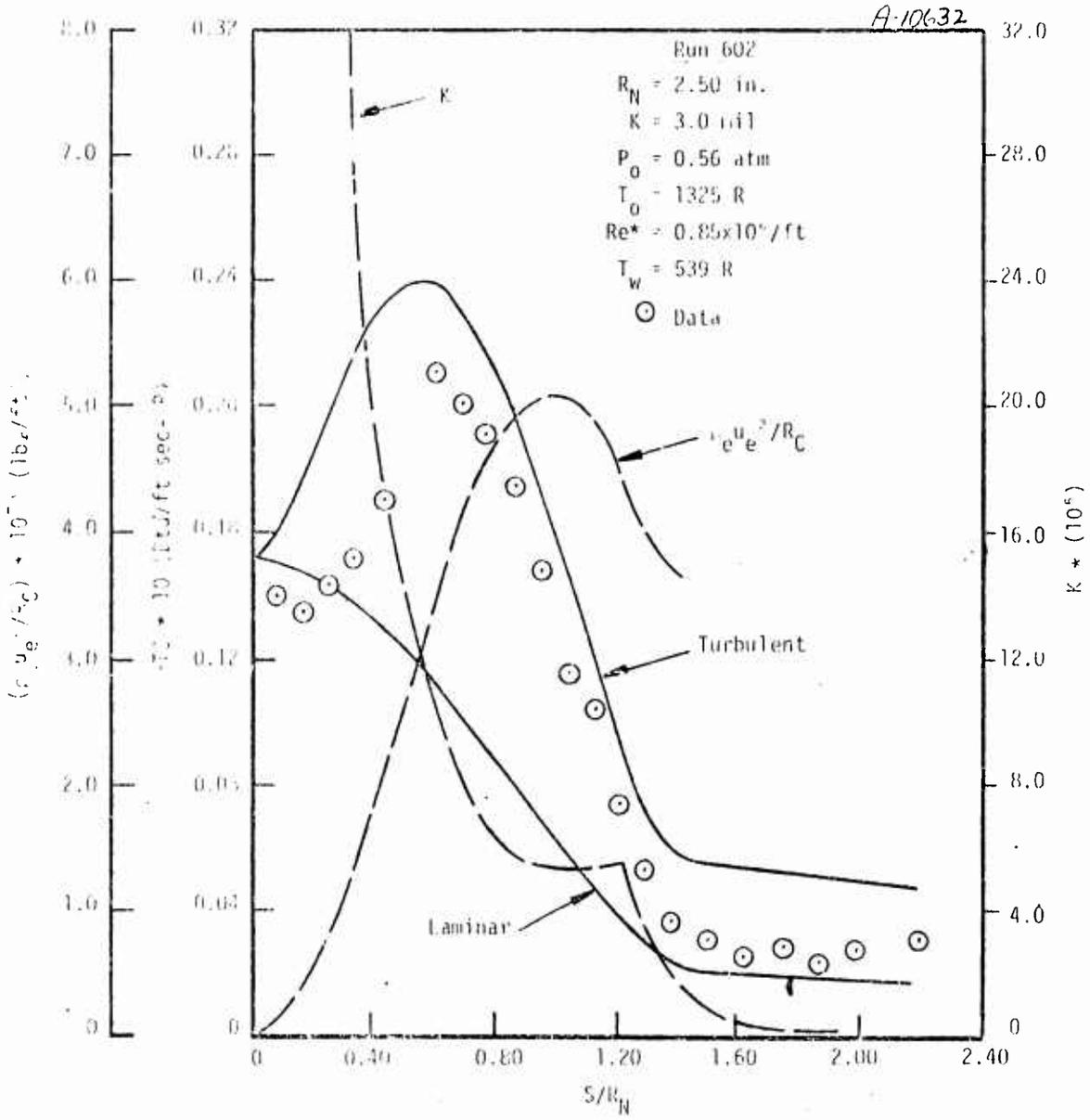

Figure 12. Distributions of heat transfer and laminarization parameters on a sphere-cone.

Since, for a plane flow with pressure gradient, there is unequivocal evidence for a "lag" effect, and since the data of Thomann (Reference 23) suggest a similar behavior when streamwise curvature is present, it is reasonable to conjecture that some aspect of this "history" of the normal pressure gradient is relevant. A simple form suggested by these considerations is

$$\Psi(S) \propto \int_{S_R}^{S} \frac{\rho_e u_e^2}{R_c} \, dS$$

where S is streamwise distance and S_R is some reference location. It is reasonable that the normal pressure gradient measured relative to that at the reference location should be in the integrand. Thus, it is postulated that the integral

$$I(S) = \int_{S_R}^{S} \left\{ \frac{\rho_e u_e^2}{R_c} - \left(\frac{\rho_e u_e^2}{R_c} \right)_{S=S_R} \right\} dS$$

is proportional to the degree of laminarization on a nosetip. Normalizing, and imposing the requirement that $\Psi(S_{F.C.}) = \Psi_{F.C.}$ gives

$$\Psi(S) = \frac{\Psi_{F.C.} I(S)}{I(S_{F.C.})}$$

With this form for Ψ, it is still necessary to choose S_R and one obvious choice is

$$S_R = S_{TRANSITION} = S_T$$

Further analysis of the data may establish a better reference location, possibly the sonic point, but the range of streamwise position in which S_R may be taken is not extremely large. The reason for this restriction is that it appears necessary that $I(S) \geq 0$ for all $S \leq S_{F.C.}$, otherwise it is doubtful that $\Psi(S)$ will follow the trend of the data.

A sample calculation, with the code modified to include $\Psi(S)$, is shown in Figure 13 for the case of a PANT Series J test. Figure 13 shows reasonable agreement between the correlation and the data, as do other test cases. The only obvious criticism is that the degree of laminarization is slightly overestimated by the correlation in the region where S is about halfway between S_T and $S_{F.C.}$. However, it is judged that I(S) is a reasonable extrapolating expression and useful for estimating nosetip laminarization.

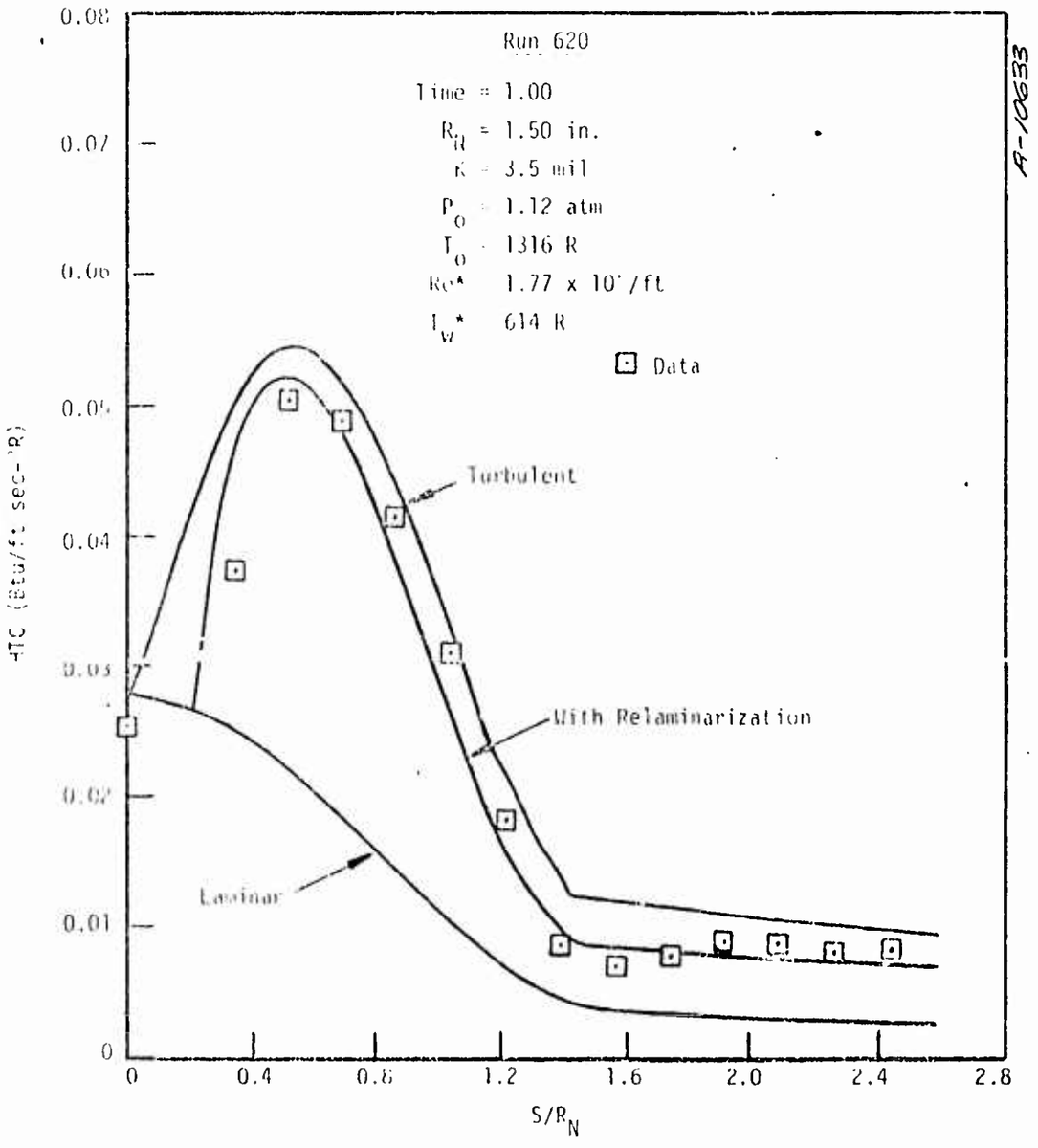

Figure 13. Comparison of relaminarization correlation and wind tunnel data.

SECTION 4

SENSITIVITY STUDY

In order to assess the impact of relaminarization on reentry nosetip shape change, the model described in the previous section was used to compute histories of heat transfer distributions over sphere cone nosetips on ballistic trajectories. Predictions were made for four reentry configurations, with and without relaminarization. Descriptions of these cases are given in Table 1. All cases were run for a peak to valley roughness height of 0.5 mils which is nominally characteristic of ATJ-S graphite as well as GE 2-2-3 carbon/carbon. As noted in Table 1, the same typical values of the ballistic coefficient and entry velocity were used for all four cases. Since nose radius and entry angle were expected to influence the overall impact of laminarization most directly, predictions were made for two values of each of these parameters. The trajectories for the two entry angles are shown in Figure 14.

Because the relaminarization model is most valid for sphere cone geometries and because this geometry is quite characteristic of the actual shape for the portion of the trajectory during which laminarization is most important, the original geometry was assumed for the entire trajectory. This approximation may slightly underestimate the influence of laminarization because the corner radius decreases in the presence of turbulent-relaminarized flow. The Sandia Nosetip Analysis Procedure (SNAP) code was run without ablation, with the wall temperature assigned at 7000°R.

Transition onset altitude and subsequent transition locations are computed in the SNAP code using the rough wall boundary layer transition criteria developed under the PANT program (see Reference 24).

$$Re_{\theta}\left(\frac{k}{\psi\theta}\right)^{0.7} = \begin{cases} 255^{*}, \text{ onset} \\ 215, \text{ location} \end{cases}$$

where

$$\psi = \frac{B'}{10} + \left(1 + \frac{B'}{4}\right)^{1/2}\frac{\mu_e}{\mu_w}$$

and

$$B' = (\rho v)_w/\rho_e u_e C_H$$

* Evaluated at the sonic point

TABLE 1

BALLISTIC AND GEOMETRIC PARAMETERS
USED IN SENSITIVITY STUDY

case	β lbf/ft^2	Ve ft/sec	γ_e degree	R_N inch	Transition Altitude ft
1	3700	22,000	-26	0.75	58,000
2	3700	22,000	-26	1.50	59,000
3	3700	22,000	-40	0.75	60,000
4	3700	22,000	-40	1.50	61,000

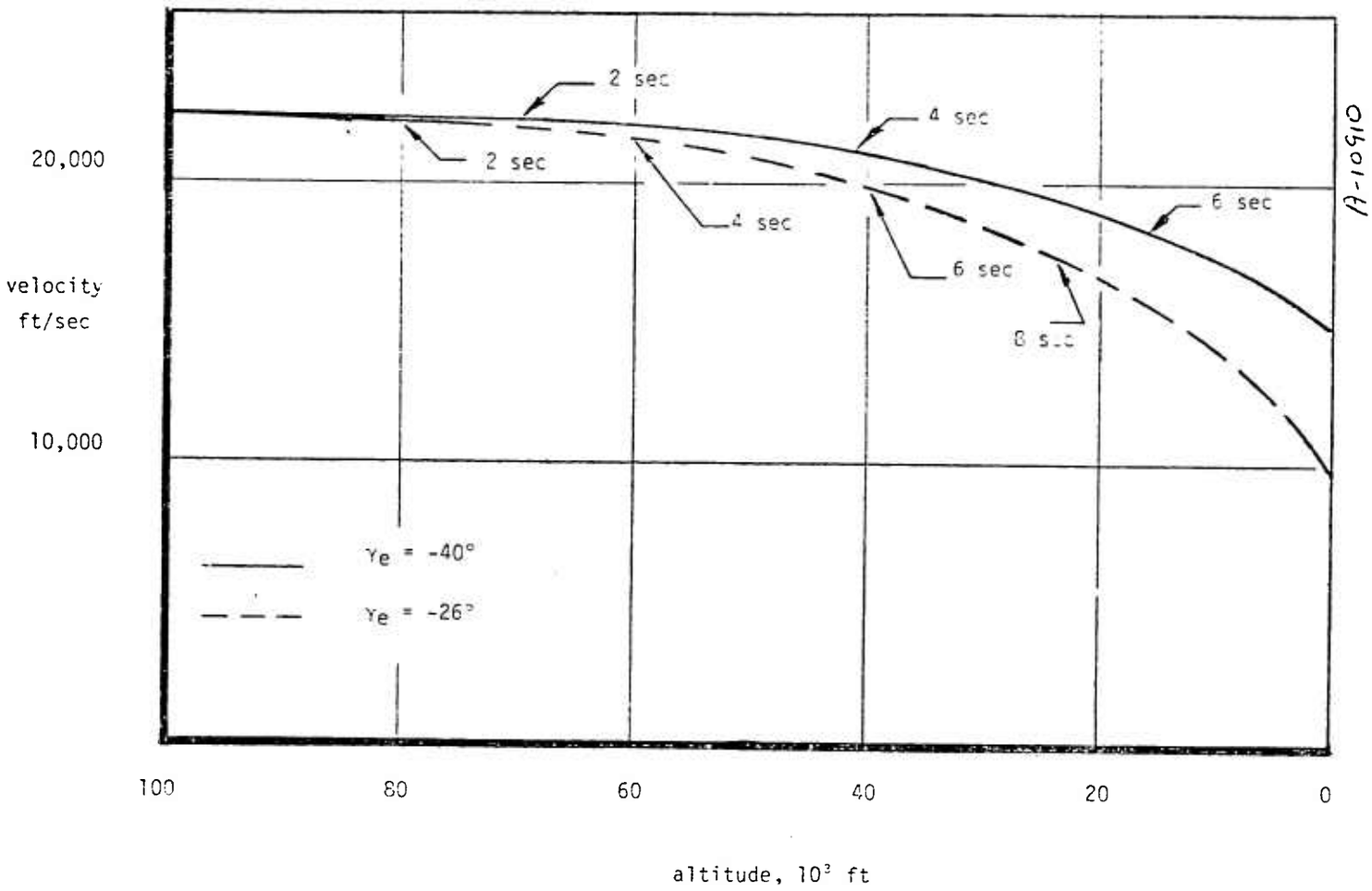

Figure 14. Trajectories used in sensitivity study.

Since ablation was not included in the present calculations, $B' = 0$ and ρ_w for pure air were used in computing ψ. This approximation yields values of ψ which are 10 percent low compared to values computed including the effects of ablation (see Figure A-20, Reference 24). This in turn implies that the transition altitudes reported herein are about 2000 ft above those which would be calculated with ablation. This has an insignificant effect on the calculation of relaminarization at any altitude and only a small effect on the integrated influence of relaminarization over the reentry trajectory.

Relaminarization has its greatest influence on the heat transfer distribution around a nosetip at altitudes just below transition onset. Figure 15 shows predicted heat transfer distributions for case 1 at 53,000 ft, about 5,000 ft below transition altitude. At the cone tangent point, $\psi = 0.77$, which is its maximum on the nosetip.

Figures 16, 17, 18 and 19 show predicted heat transfer distributions for the four cases, all at the same altitude, 41,000 ft. As expected from the cone tangent point relaminarization correlation, increasing the nose radius decreases the influence of relaminarization. It is also apparent from these four figures that for the same ballistic coefficient, entry velocity and nose radius, the entry angle has only a minor effect upon laminarization at this altitude where the velocities on the two trajectories are nearly the same.

Figures 20, 21, 22 and 23 indicate how the predicted influence of laminarization on the cone tangent point heat transfer varies with altitude for the four cases studied. The nose radius effect is as expected. Although the heat transfer on the steeper trajectory ($\gamma_e = -40°$) is considerably higher, the fractional reduction in heat transfer associated with relaminarization at any altitude is about the same for the two trajectories.

Figures 24 through 27 show the predicted influence of laminarization on the total heat transfer at the cone tangent point. Focusing on an altitude of 30,000 ft, cases one through four show a reduction of integrated heat transfer at the cone tangent point of 27, 17, 28 and 17 percent, respectively.

The reductions in heat transfer will be directly reflected in reductions in recession. Although fore cone ablation is not crucial from a recession point of view, this region of the nosetip is critical to thermostructural performance. The effects of laminarization on heat transfer are probably important with respect to thermal stress considerations and an assessment of its thermostructural impact, which was not within the scope of the present work, should be carried out.

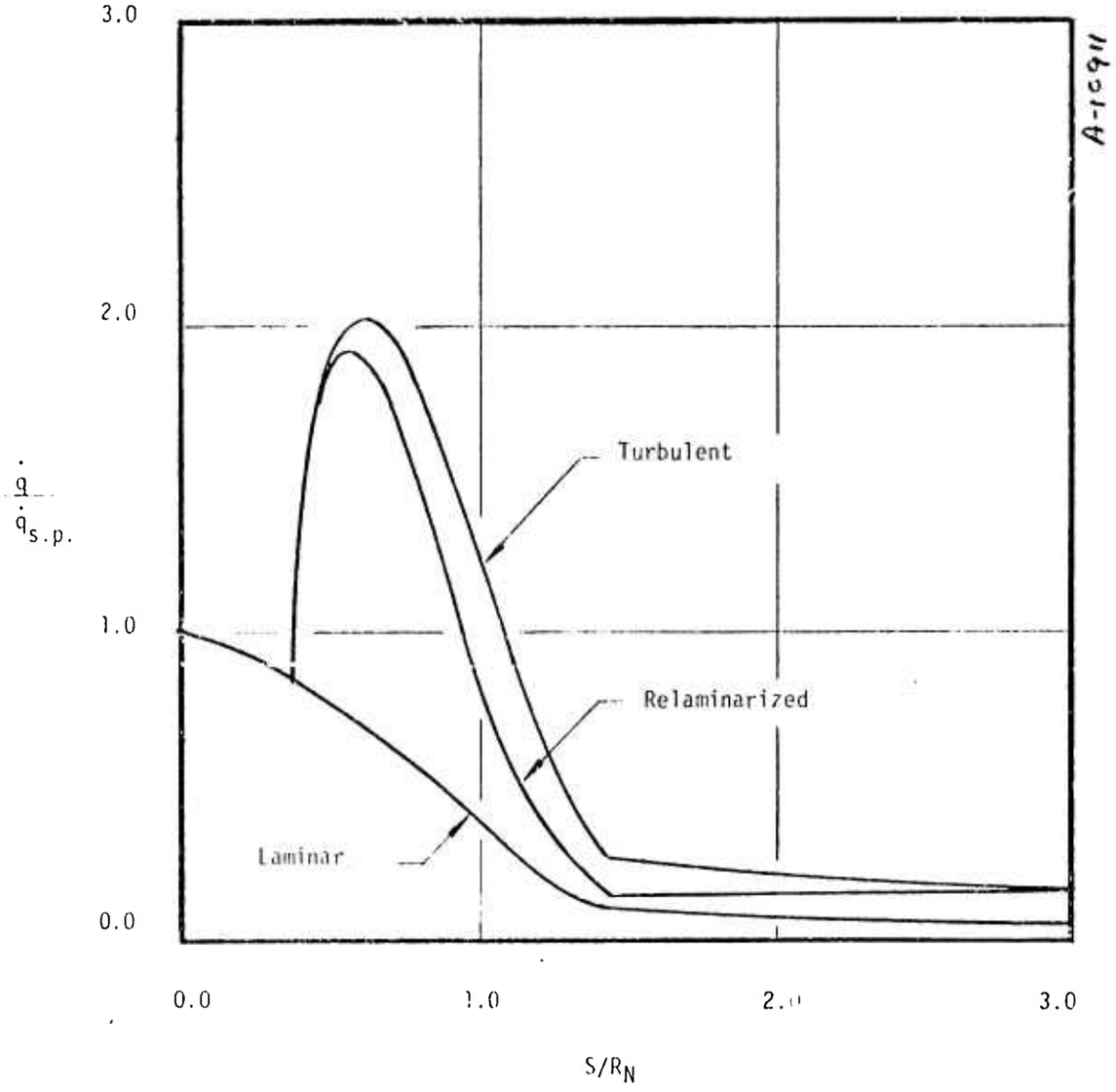

Figure 15. Nosetip heat transfer distribution with relaminarization, case 1, 53,000 ft altitude.

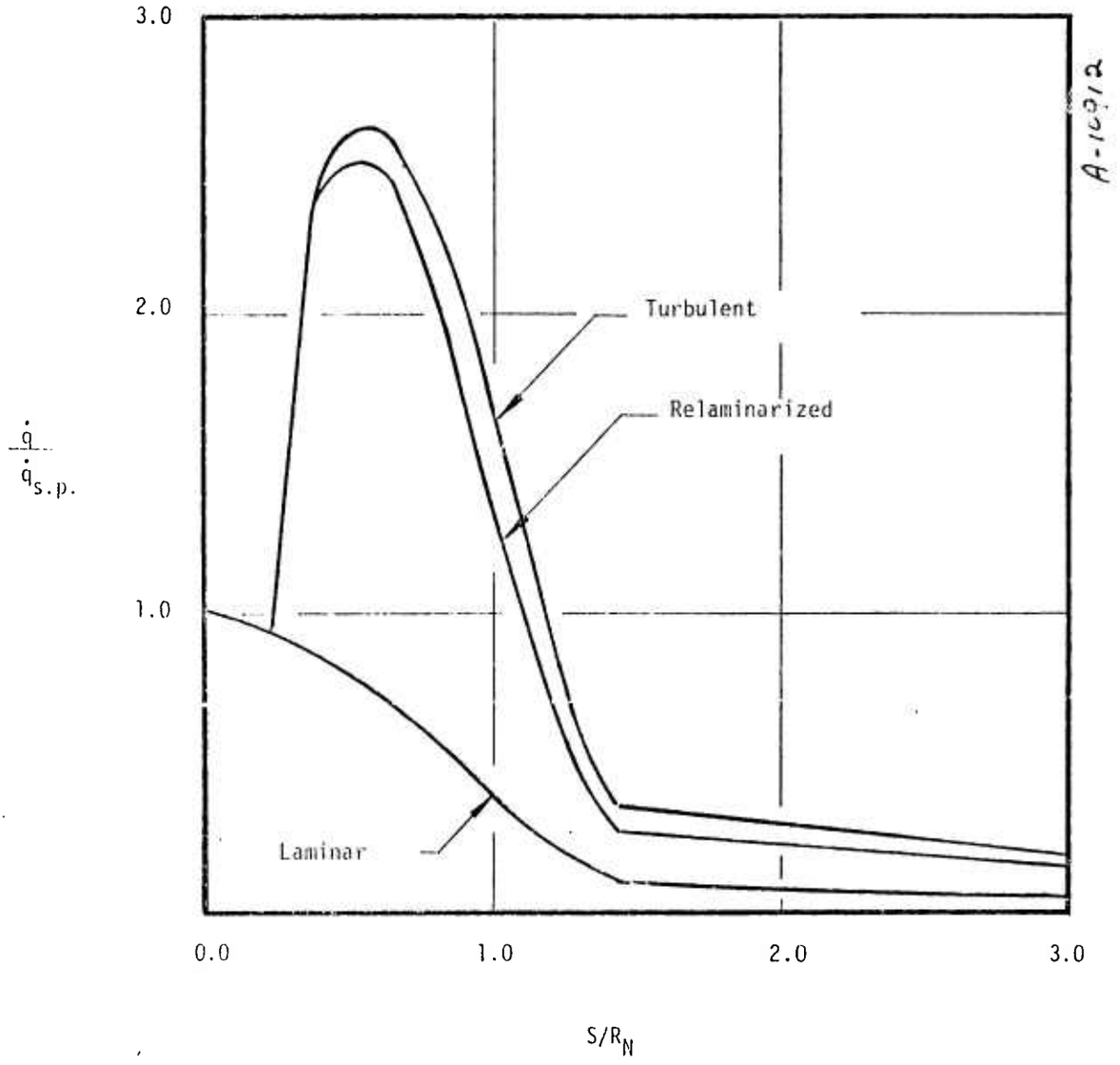

Figure 16. Nosetip heat transfer distribution with relaminarization, case 1, 41,000 ft altitude.

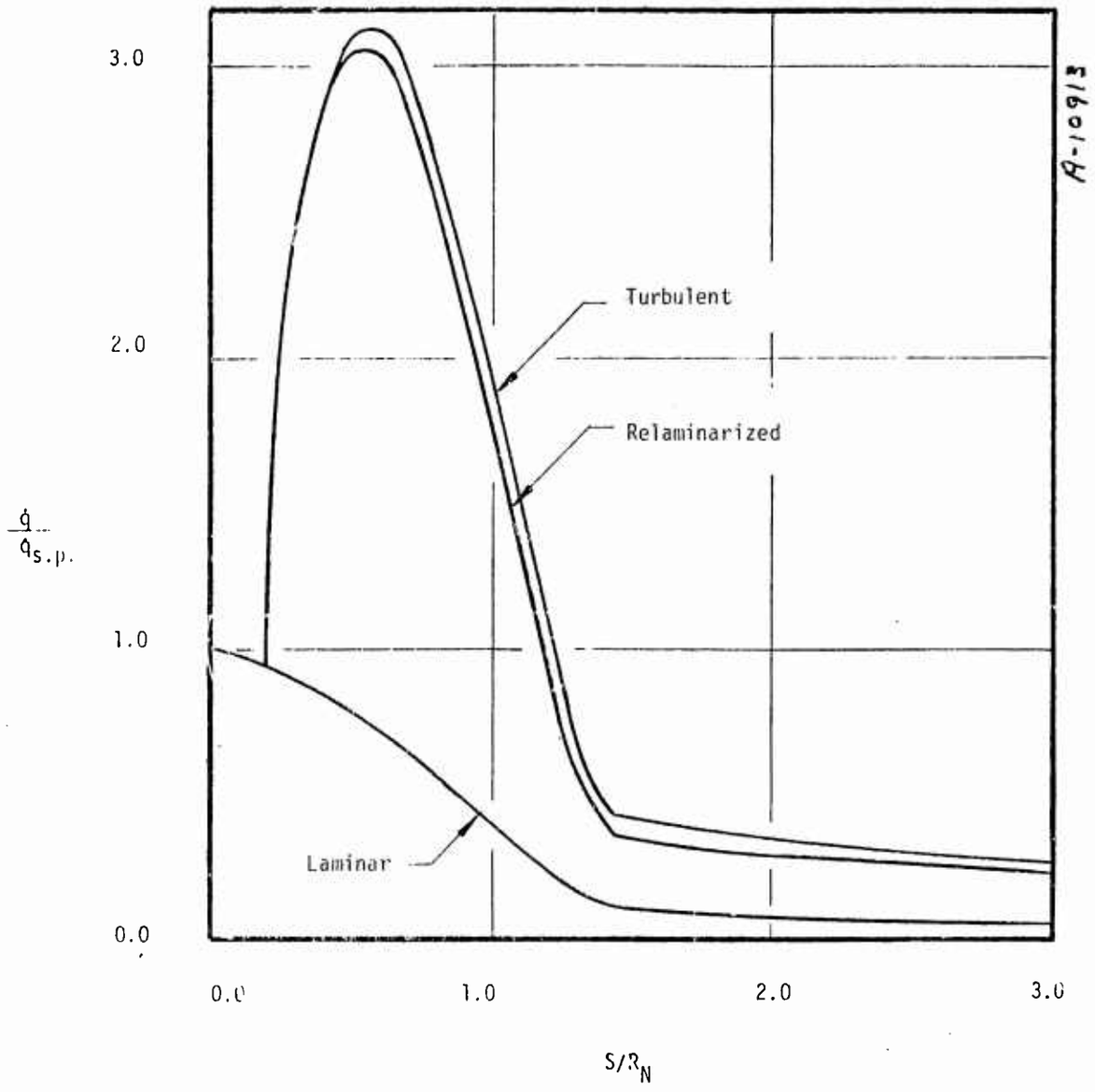

Figure 17. Nosetip heat transfer distribution with relaminarization, case 2, 41,000 ft altitude.

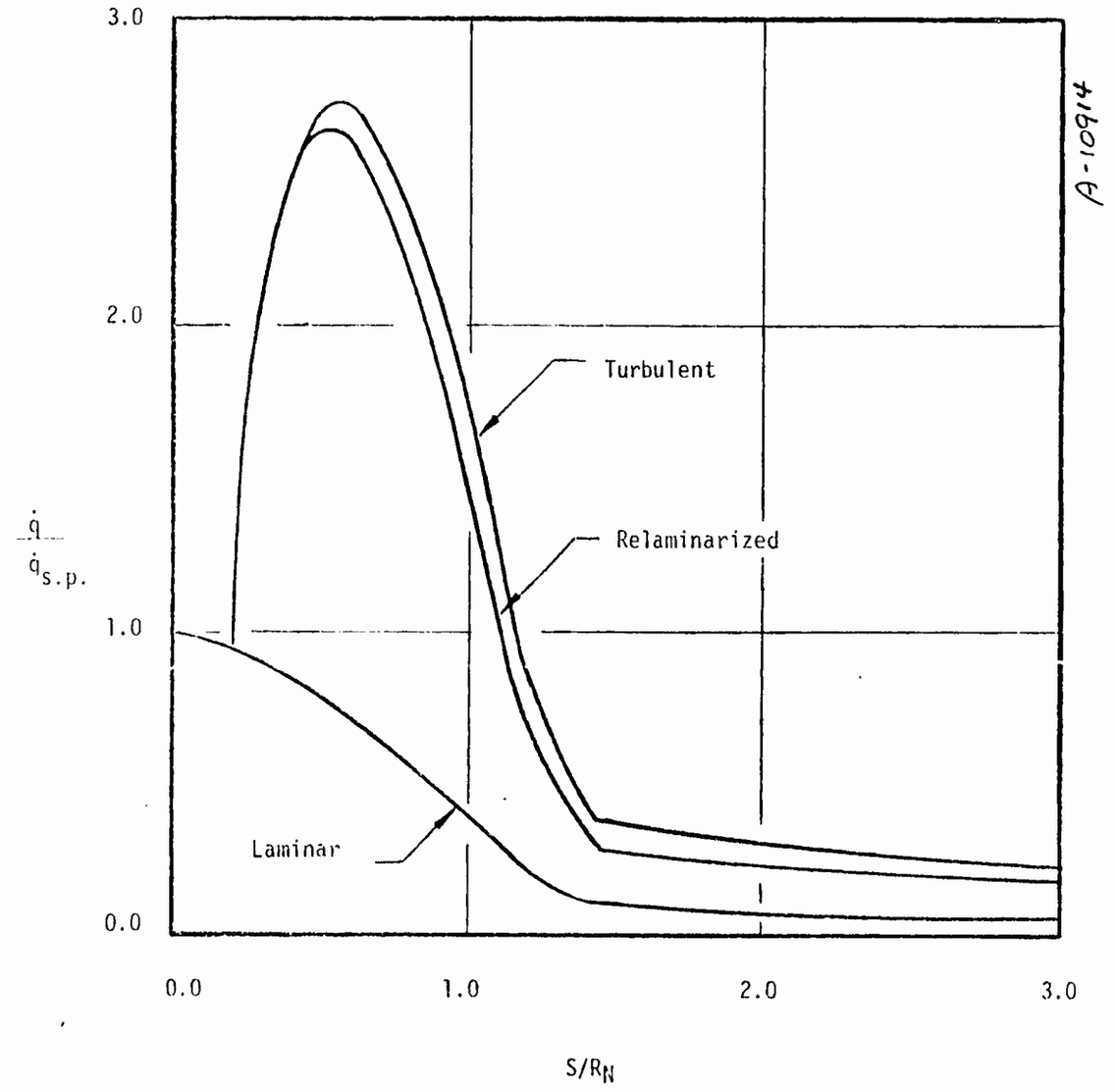

Figure 18. Nosetip heat transfer distribution with relaminarization, case 3, 41,000 ft altitude.

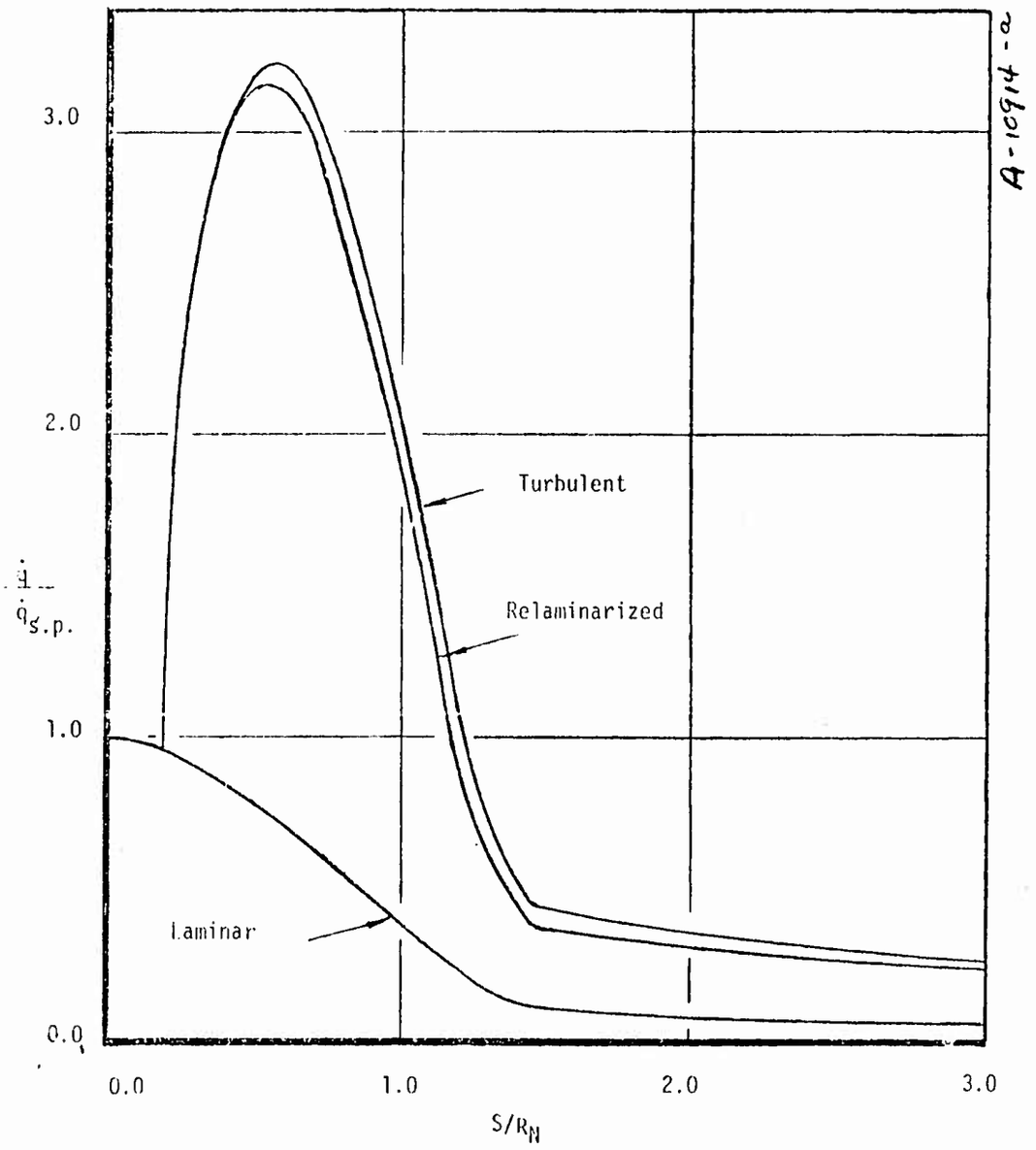

Figure 19. Nosetip heat transfer distribution with relaminarization, case 4, 41,000 ft altitude.

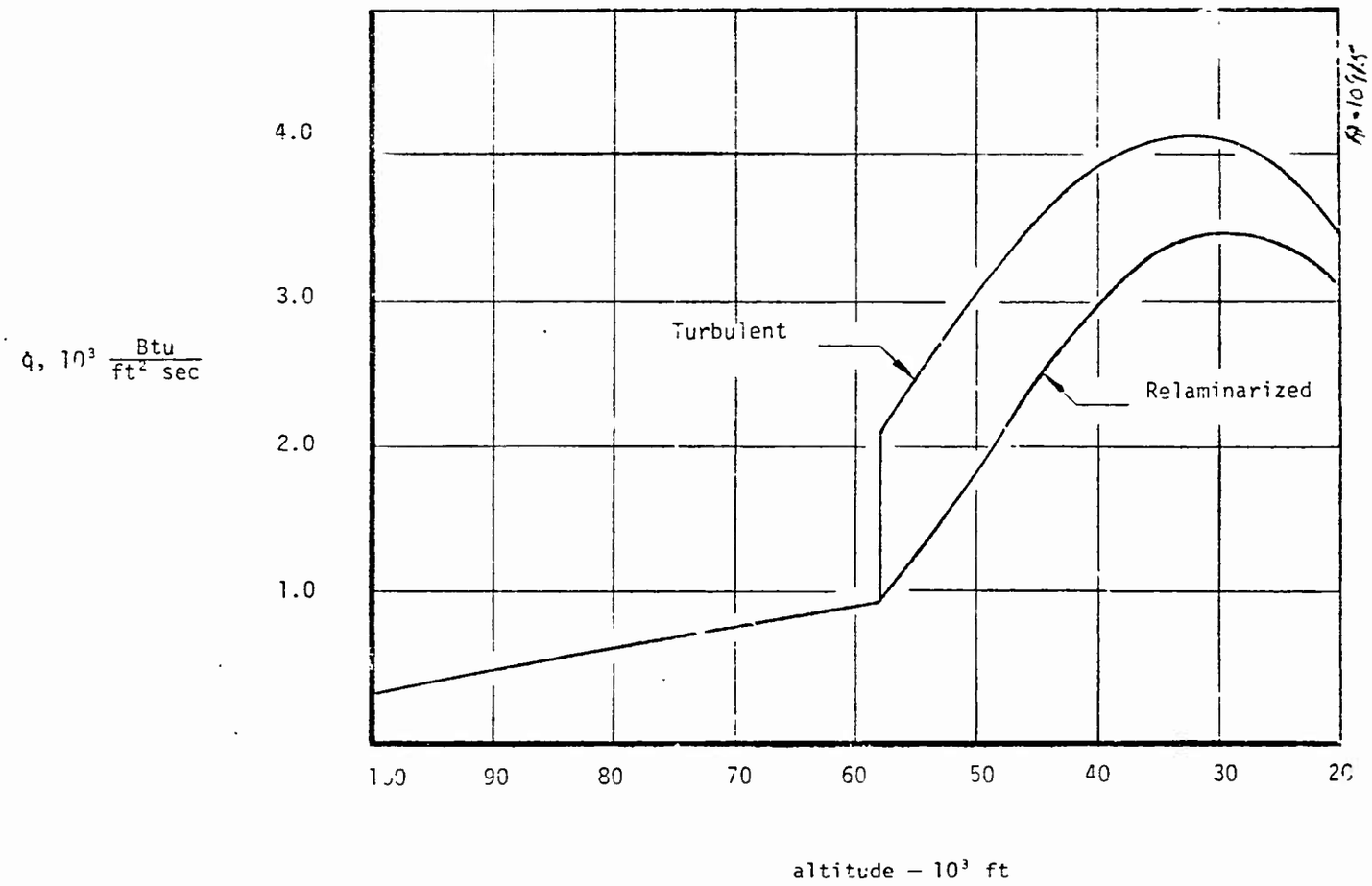

Figure 20. Fore cone heat transfer rate as a function of altitude, case 1.

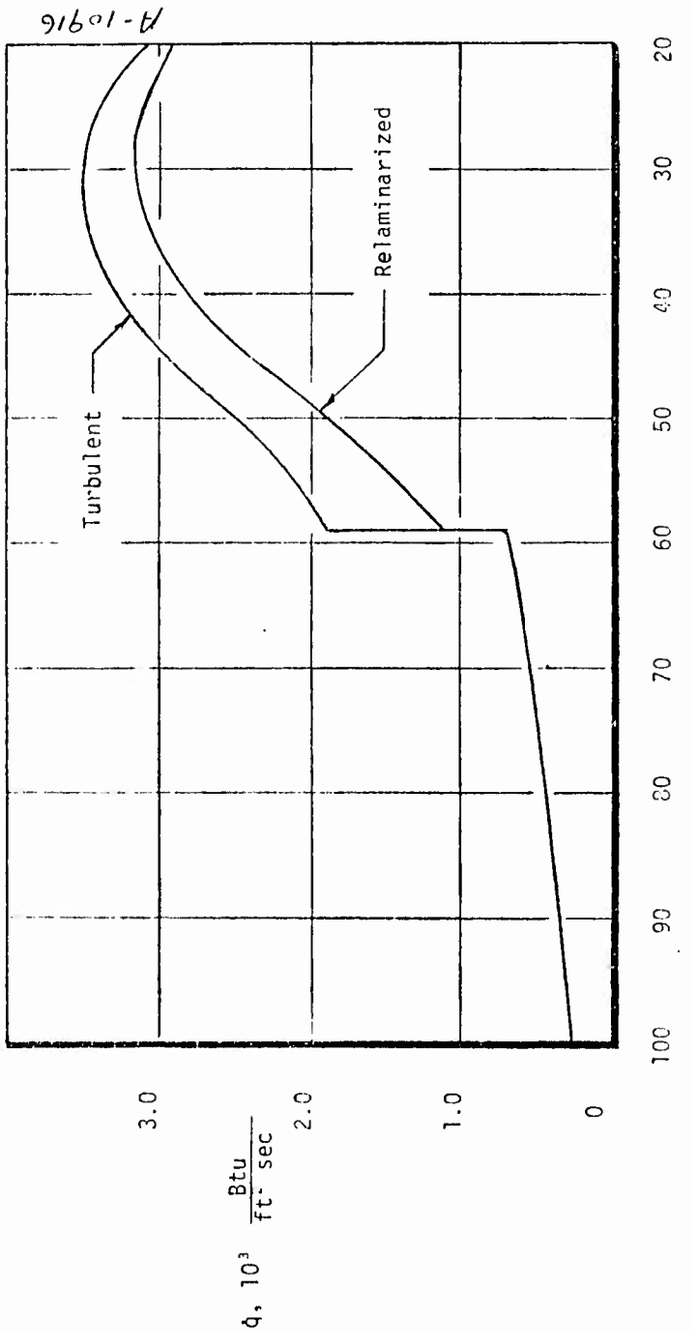

Figure 21. Fore cone heat transfer rate as a function of altitude, Case 2.

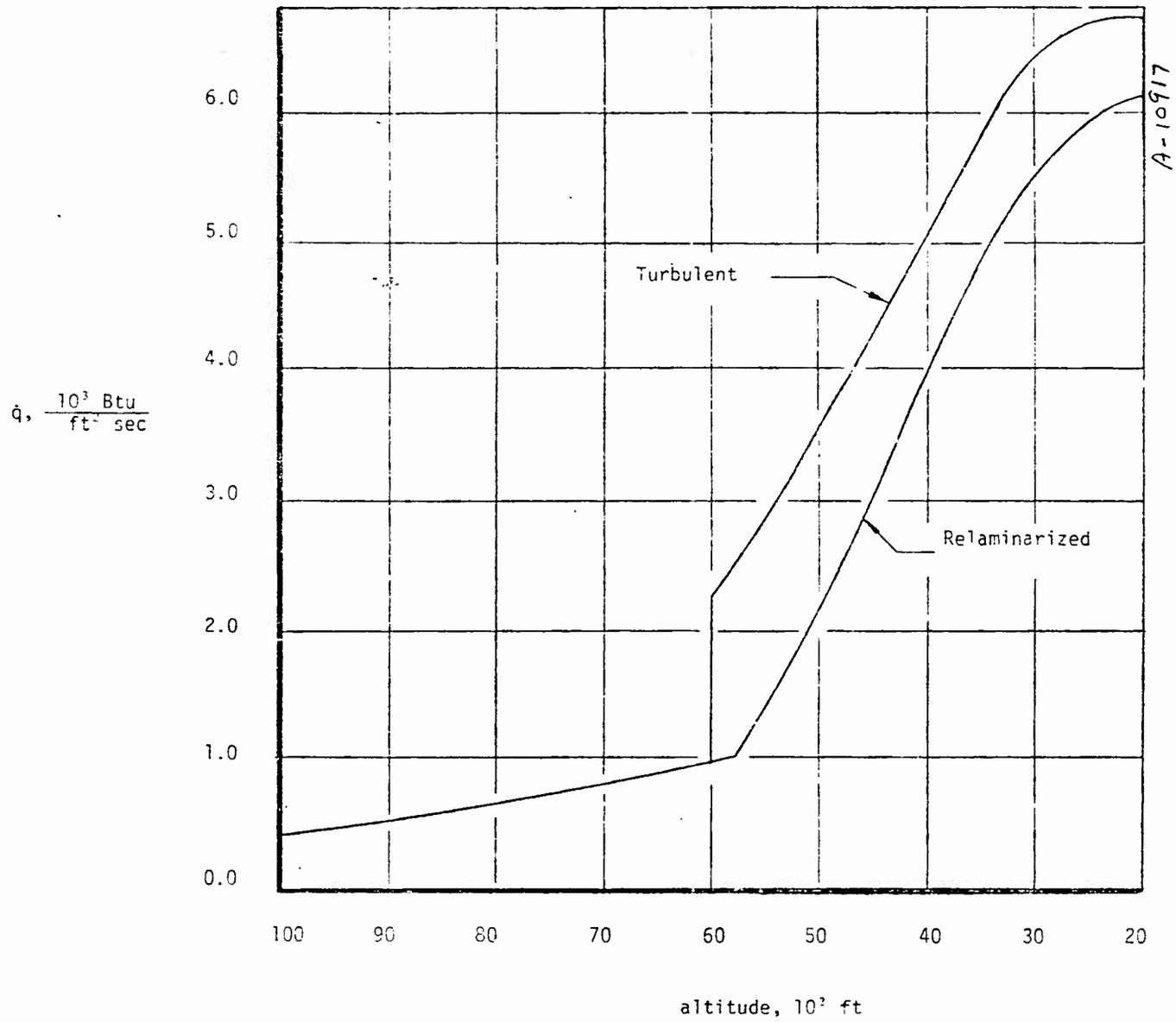

Figure 22. Fore cone heat transfer rate as a function of altitude, case 3.

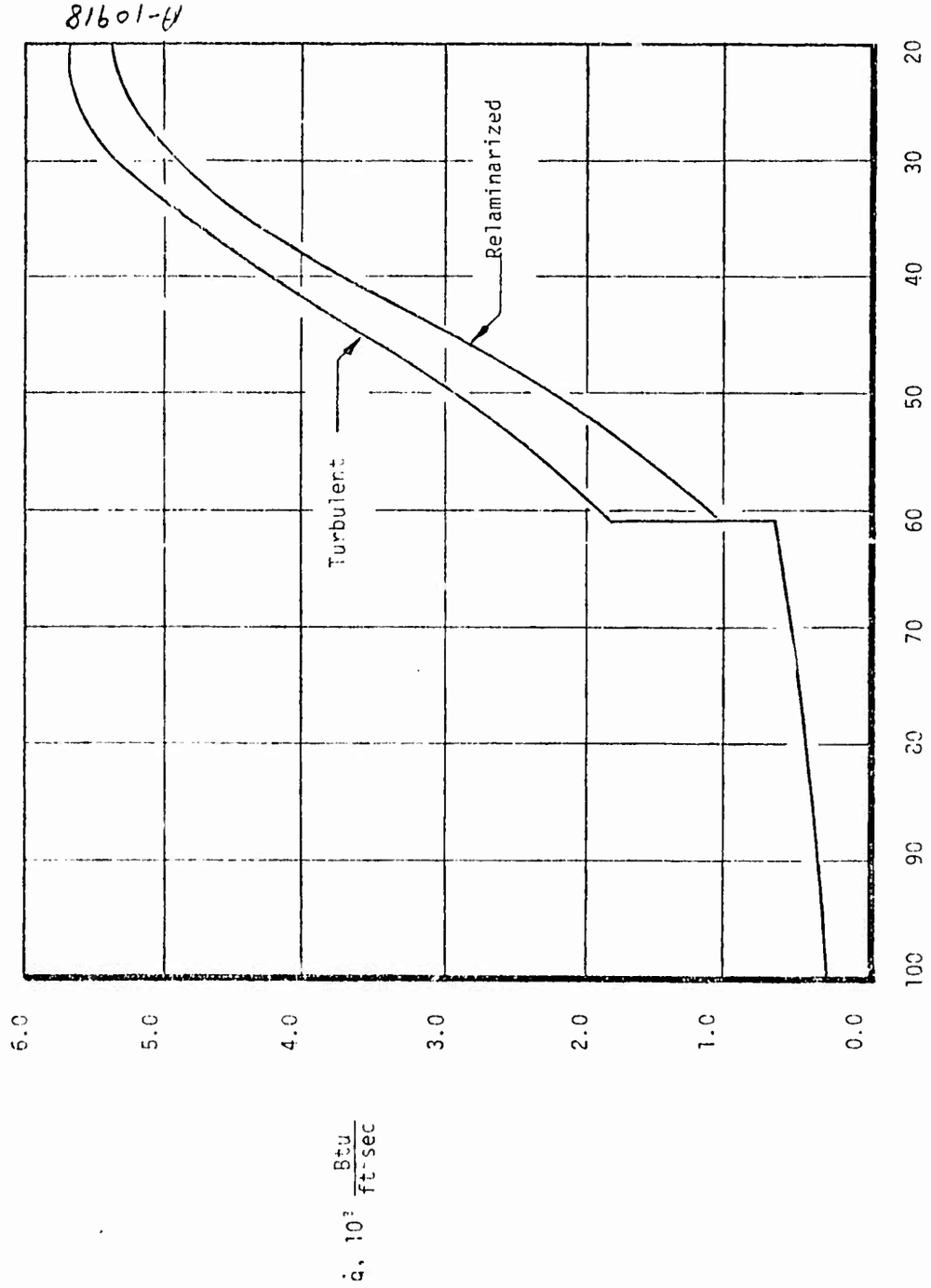

Figure 23. Fore cone heat transfer rate as a function of altitude, case 4.

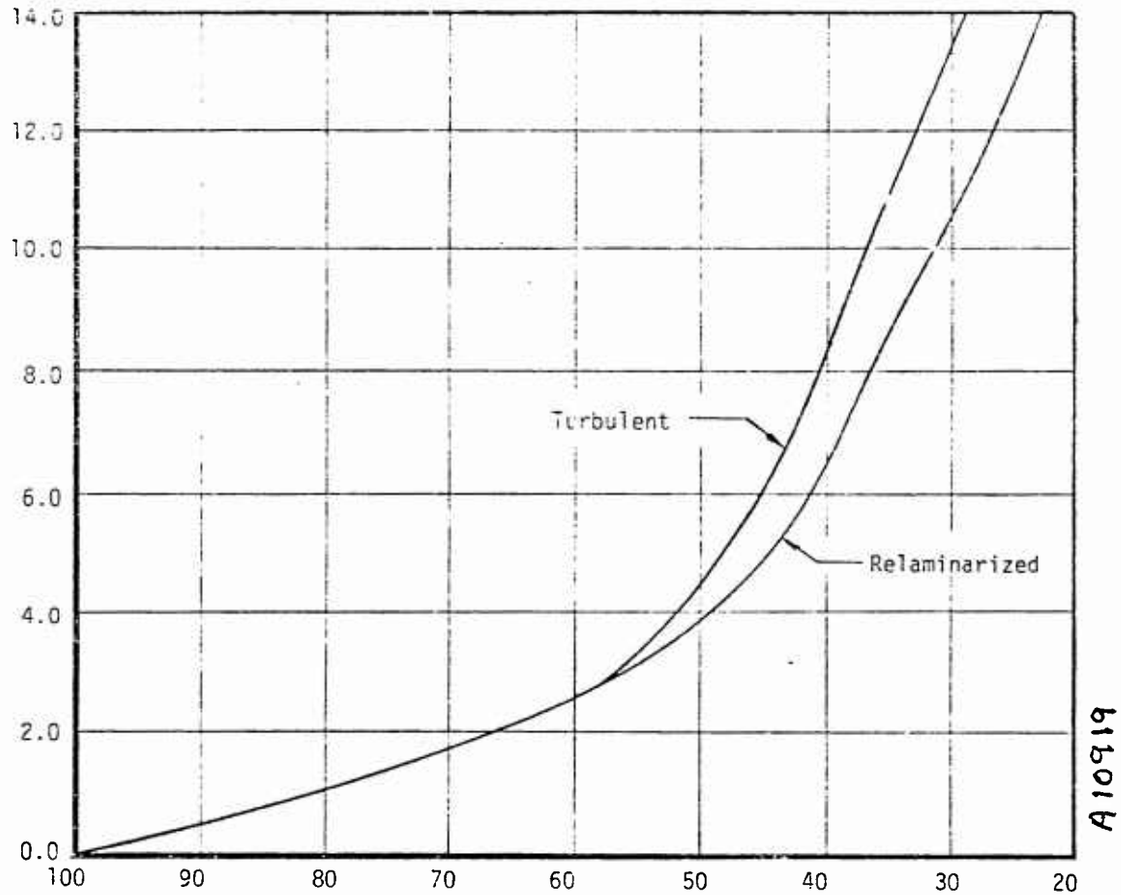

Figure 24. Compa.ison of turbulent and relaminarized integrated fore cone heat transfer, Case 1.

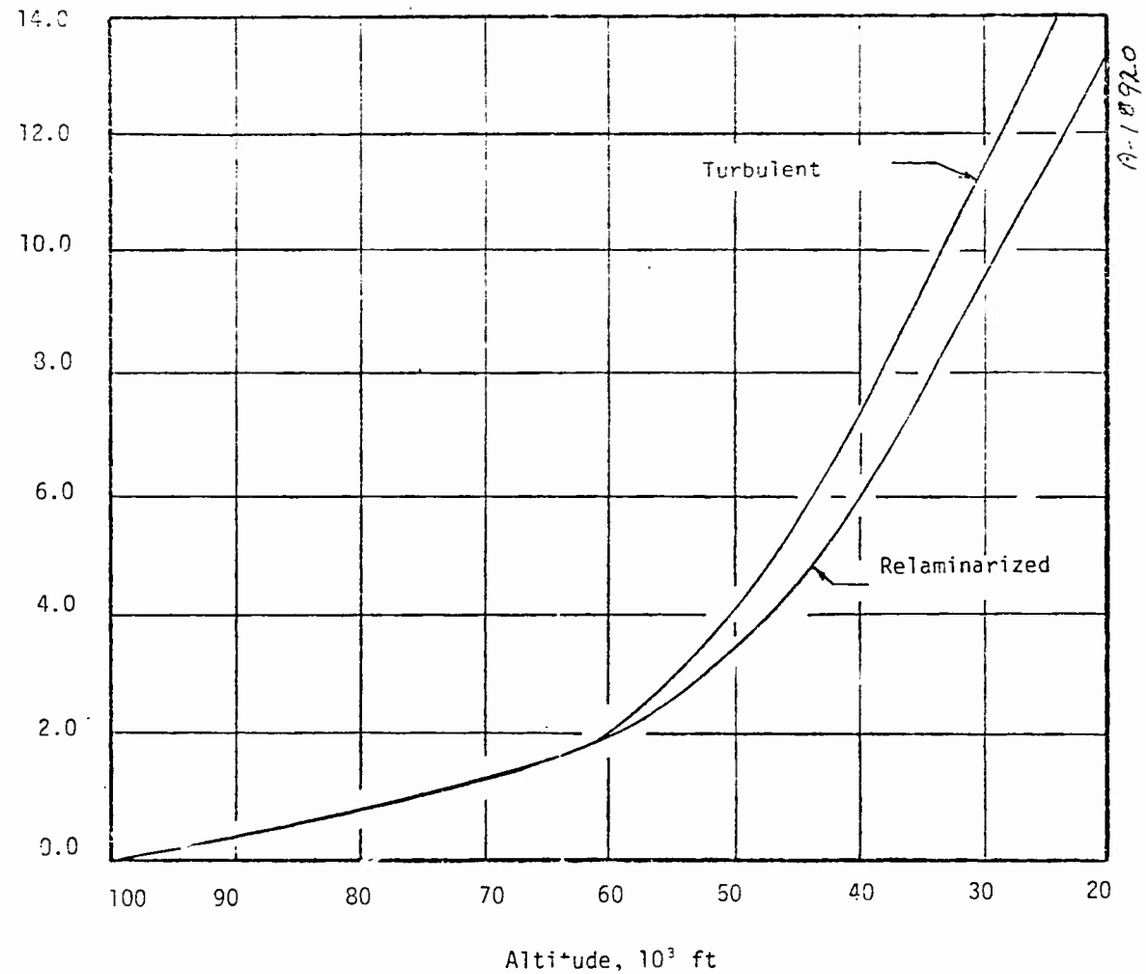

Figure 25. Comparison of turbulent and relaminarized integrated fore cone heat transfer, case 2.

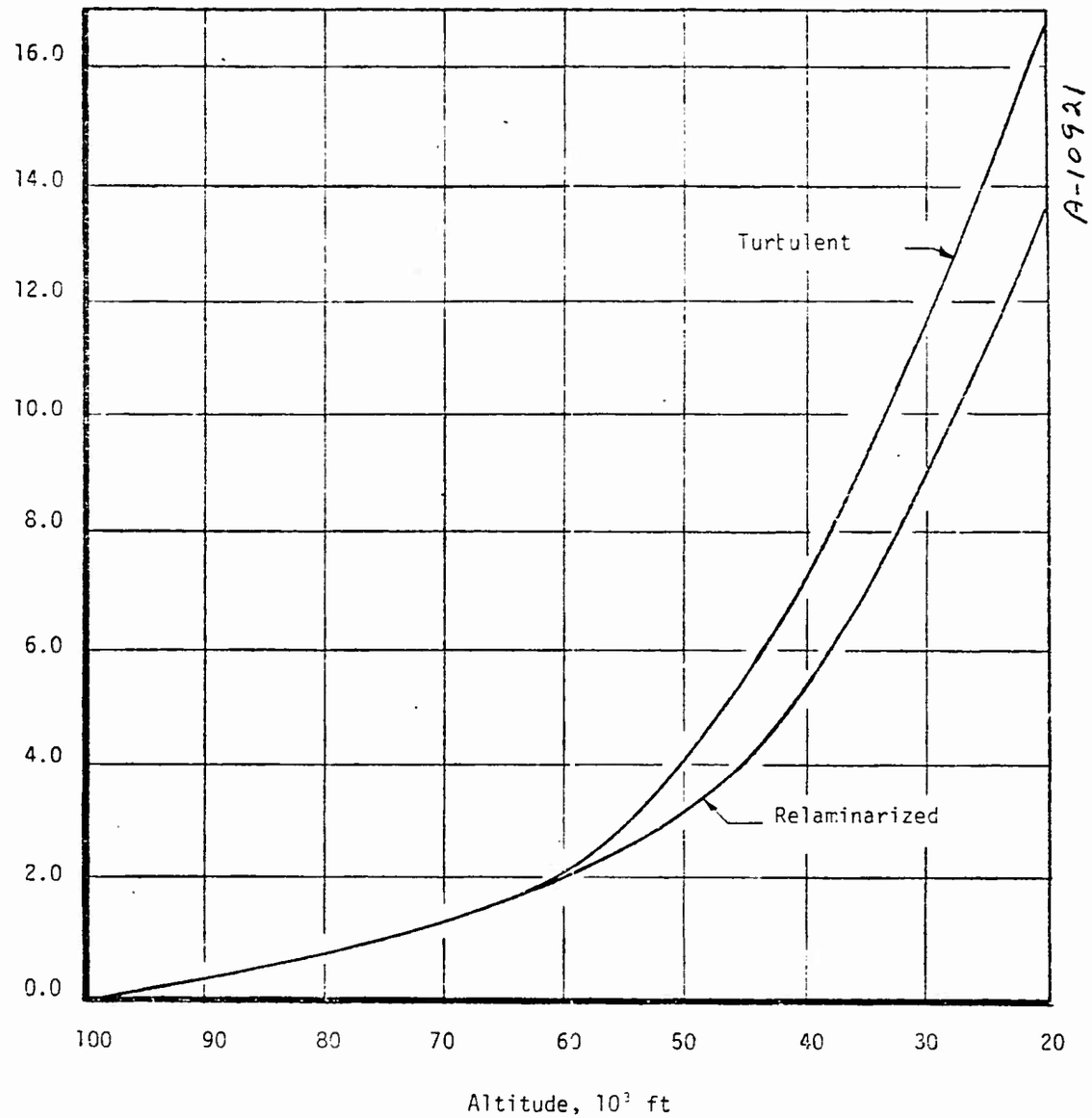

Figure 26. Comparison of turbulent and relaminarized integrated fore cone heat transfer, case 3.

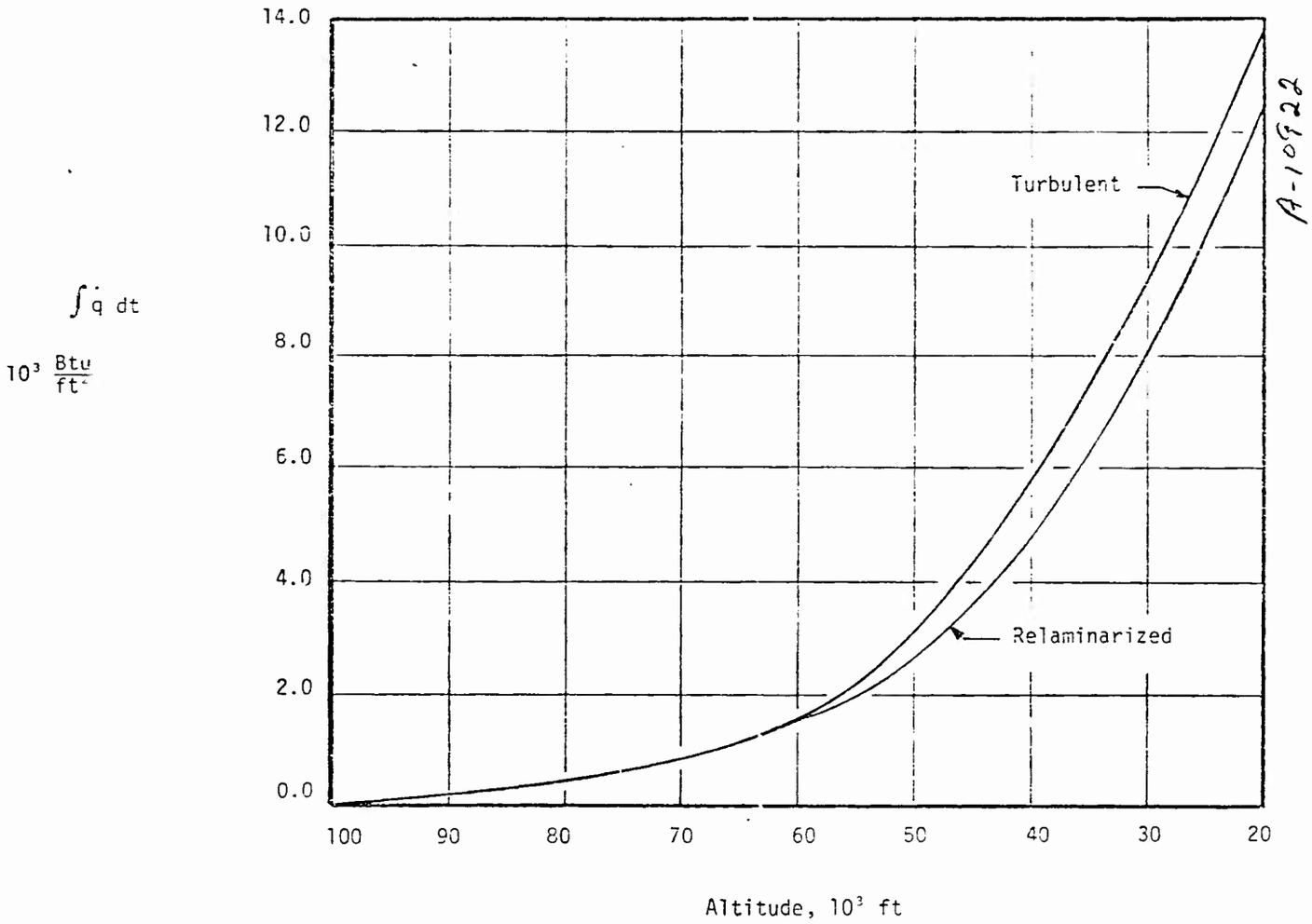

Figure 27. Comparison of turbulent and relaminarized integrated fore cone heat transfer, case 4.

SECTION 5

CONCLUSIONS

The correlation study of relaminarization of plane flows due to streamwise pressure gradient has shown the existence of inconsistencies in the experimental data. Hence, a full account of the effects of streamwise acceleration and non-equilibrium are not possible without further theoretical and experimental work to resolve these inconsistencies. However, qualitative and semi-quantitative arguments have been presented that indicate that the mechanism of nosetip laminarization is most likely associated with the effects of surface roughness and normal acceleration. As a corollary to this result, it has been shown that the commonly used streamwise pressure gradient criterion for laminarization does not give a good correlation of wind tunnel data on nosetip configurations.

An extension of an existing correlation for the degree of laminarization at the sphere-cone tangent point of a nosetip has been developed. This extended correlation predicts the distribtuion of heat transfer rate from the point of transition to downstream of the sphere-cone tangent point by means of an integral of a measure of the normal pressure gradient.

Heat transfer distributions on reentry nosetips with two nose radii and on two trajectories have been calculated in a sensitivity study of the effect of relaminarization. It has been shown that the time integral of the heat transfer rate on the fore cone of a nosetip is significantly decreased by laminarization. The reduced local heat transfer rates that result from laminarization are of importance primarily to the thermostructural performance of a nosetip, and the present results indicate the need to make a detailed study of the thermostructural ramifications of these effects.

REFERENCES

1. Wolf, C. J. and Anderson, A. D., "Critical Survey of the Literature on Relaminarization," Acurex/Aerotherm Technical Report 74-122, October, 1974.

2. Sternberg, J., "The Transition from a Turbulent to a Laminar Boundary Layer," Ballistic Research Laboratories Rept. No. 906, Aberdeen Proving Ground, Maryland, May 1954.

3. Narasimha, R. and Sreenivasan, K. R., "Relaminarization in Highly Accelerated Turbulent Boundary Layers," J. Fluid Mech., Vol. 61, 1973, pp. 417-447.

4. Baker, R. J. and Launder, B. E., "The Turbulent Boundary Layer with Foreign Gas Injection-I. Measurements in Zero Pressure Gradient," Int. J. Heat Mass Trans., Vol. 17, 1974, pp. 275-291.

5. Baker, R. J. and Launder, B. E., "The Turbulent Boundary Layer with Foreign Gas Injection-II. Predictions and Measurements in Severe Streamwise Pressure Gradients," Int. J. Heat Mass Trans., Vol. 17, 1974. pp. 293-306.

6. Deissler, R. G., "Evolution of a Moderately Short Turbulent Boundary Layer in a Severe Pressure Gradient," J. Fluid Mech., Vol. 64, 1974. pp. 763-774.

7. Deissler, R. G., "Evolution of the Heat Transfer and Flow in Moderately Short Turbulent Boundary Layers in Severe Pressure Gradients," Int. J. Heat Mass Transfer, Vol. 17, 1974, pp. 1079-1085.

8. Blackwelder, R. F. and Kovasznay, L. S. G., "Large-Scale Motion of a Turbulent Boundary Layer During Relaminarization," J. Fluid Mech., Vol. 53, 1972, pp. 61-83.

9. Patel, V. C. and Head, M. R., "Reversion of Turbulent to Laminar Flow," J. Fluid Mech., Vol. 34, 1968, pp. 371-392.

10. Badri Narayanan, M. A. and Ramjee, V., "On the Criteria for Reverse Transition in a Two Dimensional Boundary Layer Flow," J. Fluid Mech., Vol. 35, 1969, pp. 225-241.

11. Jones, W. P. and Launder, B. E., "Some Properties of Sink-Flow Turbulent Boundary Layers," J. Fluid Mech., Vol. 56, 1972, pp. 337-351.

12. Reinsch, C. H., "Smoothing by Spline Functions," Numer. Math., Vol. 10, 1967. pp. 177-183.

13. Launder, B. and Jones, W., "Sink Flow Turbulent Boundary Layers," J. Fluid Mech , Vol. 28, 1969, pp. 817-831.

14. Schlichting, H., Boundary Layer Theory, McGraw-Hill Book Co., New York, 1960.

15. White, F. M., Viscous Fluid Flow, McGraw-Hill Book Co., New York, 1974.

16. Ludweig, H. and Tillmann, W., "Untersuchungen uber die Wandschubspannung in turbulenten Reibungsschichten," Ing-Arch., Vol. 17, 1949, pp. 288-299, Summary in ZAMM, Vol. 29, 1949, p. 15, Engl. trans. NACA Tm 1285, 1950.

17. Coles, D., "Turbulent Boundary Layer in a Compressible Fluid," RAND Rept. 403-PR, 1962.

18. Blackwelder, R. F., personal communcation.

19. Deissler, R. G., personal communcation.